

A STUDY OF SOME ORGANIC AND ORGANOMETALLIC
STEREOCHEMICAL PROBLEMS BY
CRYSTALLOGRAPHIC DIRECT METHODS

A thesis presented for the degree of
Doctor of Philosophy in Chemistry
in the University of Canterbury,
Christchurch, New Zealand.

by
M.D. BRICE

1972

CONTENTS

	<u>Page</u>
CHAPTER I: Introductory Survey	
1. The Underlying Theme	1
2. Structural Study of Bis(methynyltricobaltenneacarbonyl)	2
3. Structural Study of a Cyclohexane Diol	2
4. Structural Study of Two Cyclic Sulphite Derivatives of β -pinane	4
5. Structural Study of a Cyclohexane Dione	5
CHAPTER II: Experimental Procedures	
1. Data Collection	7
2. Data Processing	10
CHAPTER III: Solution and Refinement Procedures	
1. Normalized Structure Factors	13
2. The Σ_2 Relationship	14
3. The Tangent Formula	15
4. Procedures for Phase Determination	15
5. Structure Factor Calculations and Least- Squares Refinement	21
6. The Patterson Function	23
7. Difference Fourier Synthesis	24

	<u>Page</u>
CHAPTER IV: Crystal Structure of $[\text{CCo}_3(\text{CO})_9]_2$	
1. Experimental	26
2. Solution and Refinement	28
3. Description of Structure and Discussion	30
CHAPTER V: Crystal Structure of $\text{C}_{10}\text{O}_2\text{H}_{20}$	
1. Experimental	43
2. Structure Solution and Refinement	44
3. Description of Structure and Discussion	51
CHAPTER VI: Crystal Structures of Two Isomers of $\text{C}_{10}\text{H}_{16}\text{SO}_3$	
1. Experimental	63
2. Solution and Refinement	66
3. Description of Structures and Discussion	71
CHAPTER VII: Crystal Structure of Dibenzyl Dimedone, $\text{C}_{22}\text{H}_{24}\text{O}_2$	
1. Experimental	87
2. Structure Solution and Refinement	88
3. Structure Description and Discussion	91
CHAPTER VIII: Conclusion	104
APPENDIX A: Computing System	108
APPENDIX B: Structure Factor Tables	111
REFERENCES	117

LIST OF FIGURES

	<u>Preceeding Page</u>
4.1 A Perspective View of $[\text{CCo}_3(\text{CO})_9]_2$	30
4.2 One Molecule of $[\text{CCo}_3(\text{CO})_9]_2$ viewed Normal to the Co_3 Triangle	40
4.3 A Stereoscopic View of $[\text{CCo}_3(\text{CO})_9]_2$	42
5.1 A Perspective View of the First Independent Molecule of $\text{C}_{10}\text{H}_{20}\text{O}_2$	60
5.2 A Perspective View of the Second Independent Molecule of $\text{C}_{10}\text{H}_{20}\text{O}_2$	61
5.3 A Stereoscopic View of the Contents of Two Unit Cells of $\text{C}_{10}\text{H}_{20}\text{O}_2$	62
6.1 A Perspective View of $\text{C}_{10}\text{H}_{16}\text{SO}_3(\text{A})$	71
6.2 A Stereoscopic View of $\text{C}_{10}\text{H}_{16}\text{SO}_3(\text{A})$	84
6.3 A Perspective View of $\text{C}_{10}\text{H}_{16}\text{SO}_3(\text{B})$	85
6.4 A Stereoscopic View of $\text{C}_{10}\text{H}_{16}\text{SO}_3(\text{B})$	86
7.1 A Perspective View of $\text{C}_{22}\text{H}_{24}\text{O}_2$	91
7.2 A Stereoscopic View of $\text{C}_{22}\text{H}_{24}\text{O}_2$	103

ACKNOWLEDGMENTS

I am indebted to my supervisor Professor B.R. Penfold for his advice and assistance.

Special thanks are due to Dr Ward T. Robinson for the interest he has shown and for the considerable amount of time he has spent assisting me; to Dr Jane Browning for her helpful criticism during the writing of this thesis; to my colleagues in the crystallography group for many useful discussions; and to the University of Canterbury for financial assistance.

CHAPTER 1
Introductory Survey

1.1 The Underlying Theme

The crystal and molecular structures of five compounds are described in this thesis. Of the five, one is the organometallic cobalt carbonyl cluster compound, bis(methynyltricobaltenneacarbonyl), $[\text{CCo}_3(\text{CO})_9]_2$. The other four are wholly organic and are classed as all 'light atom' structures.

The compounds studied were chosen primarily because they were suitable subjects for the use of particular techniques of structure analysis which were new to this laboratory. Therefore, although each has considerable intrinsic interest, the five compounds are not in fact chemically related.

The techniques referred to required the phasing of observed structure amplitudes using direct methods which involve statistical analyses of the X-ray reflection intensities. It was intended to develop practical procedures for applying these direct methods to crystallographic problems in this laboratory.

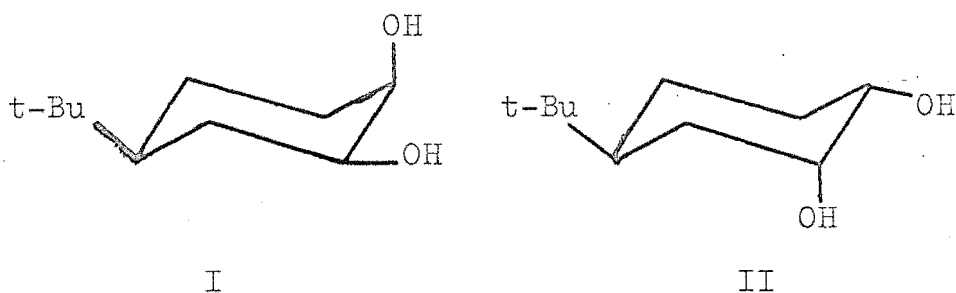
This aim has been achieved as the symbolic addition procedure and the tangent formula have been used in solving all the structures reported here.

1.2 Structural Study of Bis(methinyltricobalteneacarbonyl)

The compound $[\text{CCo}_3(\text{CO})_9]_2$ was first reported by Allegra¹, Peronaci and Ercoli who prepared it by warming bromomethinyltricobalt enneacarbonyl, $[\text{BrCCo}_3(\text{CO})_9]$, in anhydrous toluene. They assumed that it was a dimer containing two connected $-\text{CCo}_3(\text{CO})_9$ units of the type first characterised in $\text{CH}_3\text{CCo}_3(\text{CO})_9$ ². A number of further products of the reaction between $\text{YCCo}_3(\text{CO})_9$ ($\text{Y} = \text{Cl}, \text{Br}$) and arenes have been isolated, and structurally characterised³⁻⁷, and all have proved to be based on the $-\text{CCo}_3(\text{CO})_9$ structural unit containing a CCo_3 tetrahedron. Study of the detailed geometries of these molecules pointed to the desirability of a precise structure determination of $[\text{CCo}_3(\text{CO})_9]_2$. The two CCo_3 tetrahedra have been found to be linked through an extremely short, formally single, carbon-carbon bond.

1.3 Structural Study of a Cyclohexane Diol

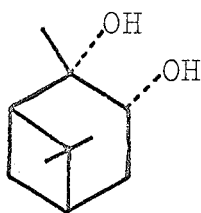
During the course of chemical studies within this department, other workers required the 1,2-cis-diols of 4-t-butyl-cyclohexane. Oxidation of 4-t-butyl-cyclohex-1-ene with KMnO_4 ⁸ resulted in the formation of two cis-diols (I and II).



The similarity of the proton magnetic resonance spectra of these two compounds and the failure of several attempts to identify them by chemical means necessitated an X-ray structural analysis. The minor product from the oxidation (MP 73-75°C) was chosen for the analysis as it exhibited better crystalline properties. With four molecules in a triclinic unit cell this problem appeared to be well suited for the symbolic addition procedure. The stereochemistry of this compound had been tentatively assigned as 4α-t-butyl-cyclohexane-1β,2β-diol(II). The structure has been found to consist of aggregates of four molecules hydrogen-bonded together to form discrete chains parallel to the crystallographic c axis.

1.4 Structural Study of Two Cyclic Sulphite Derivatives of β -pinane

Reaction of ($^+$ $_{-}$)-10 β -pinane-2,3 α -diol (III) with thionyl chloride⁹ gave a mixture of two cyclic sulphites, separable by fractional crystallisation.



III

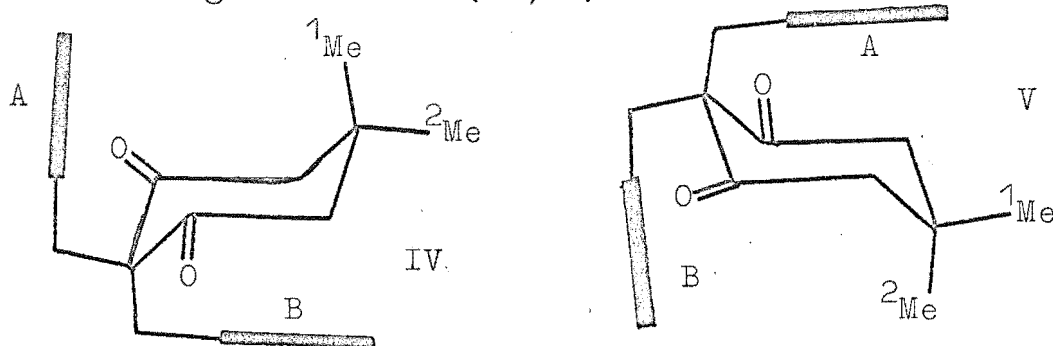
Both isomers (A, M.P. 50-52°C; B, M.P. 102-103°C) could arise if the 10 β -methyl group were cis- or trans- to the exocyclic sulphite oxygen atom.

An optically pure sample of isomer B was prepared by fractional recrystallisation and determined to be pure by proton magnetic resonance spectroscopy. This compound was used to test procedures in the application of direct methods for non-centrosymmetric crystal structures. A preliminary report¹⁰ on the structure of isomer A has been published and its structure was re-determined to obtain a result of comparable accuracy to isomer B. The two isomers were found to differ only slightly, apart from the geometrical isomerism which

was due, as expected, to the different configurations of the cyclic sulphite moiety.

1.5 Structural Study of a Cyclohexane Dione

Proton magnetic resonance studies of dibenzyl dimedone had indicated that both methyl groups were equivalent and abnormally shielded, presumably by the close proximity of the benzene rings¹¹. The suggestion had been made that this effect was due to two interconverting conformers (IV, V).



If this were the case the relative position of the benzene rings would be unchanged. An inspection of models showed that the relationships of ¹Me - to A in IV and ²Me - to B in V were the same as were ²Me to B in IV and ¹Me to A in V respectively, thus accounting for the equivalence of the Me- signals in the proton magnetic resonance spectrum. Similar arguments were used to account for the equivalence of the four ring methylene protons.

However, steric interactions between A and parts of the molecule in IV, and B and parts of the molecule in V seemed to be excessive (from models). Thus a structure determination seemed desirable to show the arrangement of groups so that the abnormal shieldings could be accounted for.

The structural study has revealed that the stereochemistry of the phenyl groups is different from that suggested.

CHAPTER II

Experimental Procedures

This chapter outlines the procedures used for the collection of all X-ray diffraction data, including intensity data and subsequent processing of this data.

2.1 Data Collection

The machine used for data collection was a Hilger and Watts computer-controlled four-circle diffractometer. Practical work on the diffractometer fell into two main sections: first, the determination of crystal orientation and refinement of unit cell and crystal orientation parameters; and second, the measurement of reflection intensities. Crystals were mounted on goniometer heads in random orientations to minimise the incidence of multiple reflection¹². For those compounds which were stable in air at room temperature samples were glued directly onto a glass fibre fixed to a head. In two cases samples which were not air stable had to be sealed within Lindemann glass capillary tubes which were then glued to the heads. In all cases efforts were made to ensure a rigid mounting. Before work commenced on the diffractometer preliminary diffraction photographs were recorded to determine approximate unit

cell dimensions and possible space groups. The orientation of the crystal on the diffractometer was determined from the setting angles of two reflections which had been absolutely indexed on a precession photograph. Unit cell and crystal orientation parameters were refined simultaneously by the method of least-squares¹³, using as observations the setting angles (ω , 2θ , and χ) of up to twelve reflections. These setting angles were obtained in one of two ways. Initially the procedure used was that of Busing¹⁴, where each reflection was centred in a 1.5 mm diameter diffracted beam collimator by manually varying ω , then χ then 2θ . Reflections were chosen and centred in such a way that the value for 2θ was obtained from the $K\alpha_1$ peak. At a later stage a routine was established in which the centring of a series of reflections was under the control of the computer. The procedure used here was different from that of Busing, in that the angles varied were φ , χ and 2θ , for bisecting mode geometry ($\theta = \omega$). The size of the diffracted beam collimator used was larger (3.5 mm) which precluded accurate resolution of the $K\alpha_1$ and $K\alpha_2$ peaks; hence the wavelength used in subsequent refinement of unit cell parameters was $K\bar{\alpha}$, the weighted mean of the $K\alpha_1$ - α_2 doublet.

The refined parameters obtained following least-squares treatment of these observations were considered to be satisfactory when no difference between observed and calculated angles for the twelve reflections exceeded 0.03° . This precision was usually readily achieved.

Neither the X-ray tube take-off angle (3°) nor source to crystal distance were changed during crystal alignment. Crystal quality was checked by determining the mosaicity, expressed as the width (in degrees) at half-height of strong low angle reflections recorded with open-counter ω -scans¹⁵. As the tube take-off angle was fixed at 3° the values for the half-heights obtained were larger than those normally obtained at lower take-off angles but values of 0.08 - 0.15° were acceptably low.

Intensity data were collected by the θ - 2θ scan technique under control of the computer. The incident beam was filtered with the appropriate β -filter. The scans were symmetric and centred on the peak position calculated from the wavelength of $K\alpha$ radiation. They were composed of steps of 0.02° in 2θ and 0.01° in ω , and suitable scan widths were determined experimentally for each crystal.

Stationary-crystal, stationary-counter background counts were measured at each end of the scan, with total background counting time approximately one-half the total scan time. The distance from the crystal to the receiving aperture of the diffracted beam collimator (DBC) was permanently fixed at 23 cm and all intensity data were collected, using a 5.0 mm DBC.

For some data sets coincidence losses in the scintillation counter were significant for some reflections. For these the scan was repeated with the incident beam attenuated with nickel foils for which the attenuation factor was subsequently determined.

2.2 Data Processing

The method of data processing was similar to that of Corfield, Doedens and Ibers¹⁶. Background scattering was considered to be a linear function of θ throughout the scan range, so that

$I = C - \frac{1}{2}(t_c/t_b)(\beta_1 + \beta_2)$, where C is the scan count, β_1 and β_2 are the first and second background counts, and t_c and t_b are the scan and background counting times.

The estimated standard deviation (e.s.d.) in the intensity I was computed as

$$\sigma(I) = [C + \frac{1}{4}(t_c/t_b)^2(\beta_1 + \beta_2) + (pI)^2]^{1/2},$$

where 'p' is a factor introduced¹⁷ to avoid overweighting strong reflections. Values for p ranged from 0.05 to 0.075 and were determined by analysis of the agreement between observed and calculated structure factors towards the end of each refinement. In all data sets weights were adjusted so that the function minimised showed as small as possible systematic dependence on $|F_0|$, $\sin \theta/\lambda$ and reflection indices¹⁸. The weights were taken as $4F_0^2/[\sigma(F_0^2)]^2$, and were adjusted by varying the value of p in the expression for $\sigma(F_0^2)$.

Normally, a number of reflections were observed more than once. This was either due to a machine malfunction or because more than one equivalent member of the form was collected.

Values of F^2 for these data were taken as the weighted mean of the individual observations. The e.s.d., $\sigma(F^2)$ was taken either as the average of the individual e.s.d.'s of equivalent reflections or as a value estimated from the range of F^2 values of equivalent reflections, whichever was larger¹⁶. Finally, all e.s.d.'s were multiplied by $(N/OBS)^{\frac{1}{2}}$, where N was the standard number of equivalent reflections measured and OBS was the number actually recorded¹⁹.

Absorption corrections could be applied at this stage with a spherical approximation to the crystal shape, or applied at a later stage, using Gaussian integration. Input to the absorption program, DABS, consisted of the indices of the boundary faces of the crystal with perpendicular distances of these faces from an arbitrary origin in the crystal. Checks could be made that the size and shape of the crystal were correctly defined by plotting the calculated points of intersection of all the boundary faces. This was a standard procedure.

CHAPTER III

Solution and Refinement Procedures

All structures described were solved by the use of direct methods, the symbolic addition procedure (sum of angles formula in the non-centrosymmetric case), the tangent formula and Fourier syntheses. They were refined by full-matrix least-squares techniques. Some details of these methods are outlined in this chapter.

3.1 Normalized Structure Factors

Normalized structure factor magnitudes, $|E|$ are calculated in such a way that

$$\langle |E|^2 \rangle = 1 \quad (1)$$

They are defined by the expression²⁰

$$|E| = \left[\frac{K(\sin^2 \theta)}{N \tau \sum f_i^2 \sin^2 \theta \lambda^{-1}} \right]^{\frac{1}{2}} |F_0| \quad (2)$$

where τ is a factor to allow for systematic absences, N is the number of atoms in the unit cell, each with scattering f_i . $K(\sin^2 \theta)$ is the normalization curve which places $|F_0|$ on an absolute scale for point atoms at rest. It is obtained from the expression;

$$K(\sin^2 \theta) = \exp(A_0 + A_1 \sin^2 \theta) \quad (3)$$

where A_0 and A_1 are defined by the Wilson plot method²¹ using the expression;

$$\log_e \frac{\langle \sum_{m \tau}^R \sum_i^N f_i^2 \sin^2 \theta \lambda^{-1} \rangle_q}{\langle \sum_m |F_0|^2 \rangle_q} = A_0 + A_1 \langle \sin^2 \theta \rangle_q \quad (4)$$

R is the number of reflections in range q , m is the multiplicity and the other terms are as defined above. An overall isotropic temperature factor, B and an overall F_0 -scale, K' , can then be obtained:

$$B = A_1 \cdot \lambda^2/2 \quad (5)$$

$$K' = \exp(A_0/2) \quad (6)$$

3.2 The Σ_2 Relationship

To implement any of the phase determining formulae it is necessary to obtain a listing of all triplets of reflections which satisfy the Σ_2 relationship²², i.e.

$$\underline{h} = \underline{h-k} + \underline{k} \quad (7)$$

This list is restricted, as interest is concentrated on those data with $|E|$ greater than some minimum value, estimated by experience, and usually 1.5. These triplets are used to implement the relationship

$$sE_h \approx s \sum_{k_r} E_k E_{h-k} \quad (8)$$

where s means "sign of" and the sum is over a restricted range r . This is the basis of the symbolic addition procedure for centrosymmetric crystals. These triplets are also used in implementation of the sum of angles formula²⁰ for noncentrosymmetric crystals

$$\varphi_h \approx \langle \varphi_k + \varphi_{h-k} \rangle_{k_r} \quad (9)$$

where the average is again taken over a restricted range and φ_h is the phase angle of the reflection hkl .

3.3 The Tangent Formula²⁰

For both centrosymmetric and noncentrosymmetric crystals

$$\tan(\varphi_h) \approx \frac{\sum_{k_r} |E_k E_{h-k}| \sin(\varphi_k + \varphi_{h-k})}{\sum_{k_r} |E_k E_{h-k}| \cos(\varphi_k + \varphi_{h-k})} \quad (10)$$

3.4 Procedures for Phase Determination

3.4.1 Centrosymmetric crystals

The symbolic addition procedure²⁰ was used, as applied by program SAP. Three operations are performed; selection of origin-defining reflections, the estimation of tentative signs, and the determination of final signs.

The origin of a centrosymmetric crystal structure²³ is fixed by specifying the structure factor signs of three, two, one, or zero linearly-independent reflections, according to the type of space group. In making these assignments the largest suitable $|E|$ should be used. The choice will also be partly determined by the extent to which a particular reflection enters into triplets, as determined by the Σ_2 relationship.

After the phase specifications which define the origin have been made, some additional symbols are assigned in a step-wise fashion, as required, to other large $|E|$ reflections which enter into a number of Σ_2 relationships. The signs of other reflections are determined gradually, by successive application of the Σ_2 relationship, and the estimated sign or symbol is accepted only when the corresponding sum given by the expression

$$\sum_{k_r} \sigma_3 \sigma_2^{-3/2} |E_h| E_k E_{h-k}| \quad (11)$$

where

$$\sigma_n = \sum_{i=1}^N Z_i^n \quad (12)$$

is above a specified limit.

Attempts are then made to evaluate the signs of the symbols, by comparing the accumulated sums given by

expression (11) for all the possible symbols. If there is a consistent indication from several reflections that one of the symbols or symbol products is equivalent to one of the signs, then the absolute value of the symbol is determined (either + or -). The final sign of each reflection is determined by substituting the sign of the symbol and adding the sums given by the expression (11). The final sign is accepted only when the total sum is above a minimum acceptable limit.

Using the $|E|$ whose signs have been determined, Fourier maps are calculated with these $|E|$ as coefficients, generally using ten to fifteen of the largest independent $|E|$ per atom in the asymmetric unit. In a correct E-map the top peaks will give a chemically reasonable structure, although variation in the sign of one or more of the symbols may be required before the correct structure is revealed.

In some cases, the tangent formula can be used to increase the number of reflections whose signs have been determined for inclusion in the calculation of the E-map.

3.4.2 Noncentrosymmetric crystals

The procedures used are similar in some respects to those used for centrosymmetric crystals. The origin is specified in the same way, and in addition, the

enantiomorph has to be defined^{24,25}. The enantiomorph is determined by the assignment of a sign to a particular linear combination of phases which satisfies the definition of an invariant (or semi-invariant, when appropriate)²⁶. The magnitude of this linear combination of phases must not be near 0 or π .

The sum of angles formula (expression 9) is now used to assign some additional symbols to other large $|E|$ as needed, which enter into many combinations as required by expression (9). This formula may now be used to determine the phases of a majority of the remaining large $|E|$ in terms of the phase specifications and unknown symbols. The restriction to large $|E|$ ensures that the probability of a phase assignment made at this stage being correct, is acceptably high.

Trial numerical values are assigned to the unknown symbols and the tangent formula (10) is used to refine these phases and to estimate new phases in a reiterative procedure. That is, knowing the phases of reflections k and $h-k$ it is possible to estimate the phase of reflection h . The number of triplets is initially very small, i.e. one, and such a determination is termed an extension. However, the number of known phases quickly increases, hence increasing the number of contributors to expression (10). It is

usual practice to include only reflections with high $|E|$ values at the initial stages and then increase the number of contributors by lowering the threshold as the extensions progress. This procedure has the advantage of refining the phases of the statistically more reliable reflections before they are used to phase reflections with lower $|E|$ values.

If the sum of the squares of the quantities $|E| \cos \varphi_h$ and $|E| \sin \varphi_h$, obtained from the numerator and denominator of expression (10), are scaled by matching their average to the average of the corresponding set of observed $|E|_{\text{obs}}^2$ values, a set of calculated $|E|^2$ values is obtained. These can be used to calculate an R-index²⁰ defined by

$$R_{\text{Karle}} = \frac{\sum_{k_r} ||E|_{\text{obs}} - |E|_{\text{calc}}|}{\sum_{k_r} |E|_{\text{obs}}} \quad (13)$$

A value in the range 0.2-0.3 for this R will usually lead to a correct solution.

In applying the tangent formula a number of tests can be used to ensure that phases which behave abnormally will not continue to be used in the phasing process. The principle test is to ensure that the calculated normalized structure factor is greater than

a specified acceptance limit. A value of 0.4 or 0.5 for the acceptance limit is usually satisfactory. A second test is to check if during three successive iterations each of the incremental changes in phase does not exceed a specified maximum, usually about 0.7

π . This is to reduce the effect of individual phase oscillation. In centrosymmetric space groups and in some zones and lines of noncentrosymmetric data sets, phases are restricted to values of 0.0 or 1.0

π , or 0.5 or 1.5 π . A further check can be made to see if the phase of a reflection which belongs to one of these classes is within a permissible range of the restricted value. This specified range is usually about 0.4 π . A final test can be made by checking the number of contributors to a phase assignment. For the centrosymmetric case, a minimum of two is usually satisfactory. However, in the noncentrosymmetric case this limit sometimes has to be lowered to one in the early stages and increased to three or four later in the extension process, after sufficient phases have been assigned.

The calculation of the E-map is the same as in the centrosymmetric case. The number of input data is, however, usually greater. In maps which are incorrect, only parts of the structure may appear and, in general,

the arrangement of peaks does not make good chemical sense. A partial structure can be used to provide starting phases for the tangent formula in a cycling procedure²⁷.

3.5 Structure Factor Calculations and Least-Squares Refinement

Positional parameters of atoms, located by inspection of the E-map, along with thermal parameters were refined by the full matrix least-squares method. Further atoms were located from difference Fourier syntheses and the least-squares procedure repeated.

The general expression for the structure factor is

$$F_c(S) = \sum_i^N f_i(S) \cdot T_i(S) \cdot \exp(2\pi i S r_i) \quad (14)$$

where $f_i(S)$ is the atomic scattering factor, $T_i(S)$ is a function describing the thermal motion of the atom nucleus, r_i is the vector representing the position of atom i in the unit cell and S is the scattering vector. Structure factor calculations as performed by program CUCLS use approximations for the first two components of expression (14).

(1) $f_i(S)$. Tabulated values of atomic scattering factors, calculated for a hypothetical atom in the ground state and with a spherically symmetric electron density were used in all cases. These atomic

scattering factors were taken from the tabulations of Cromer and Waber²⁸ or of Cromer and Mann²⁹, but those for hydrogen were taken from Stewart et al.³⁰. The effects of anomalous dispersion were allowed for with corrections made to F_c ³¹ in the following way. If f_0 is the normal scattering factor, that for an anomalous scatterer may be written as;

$$f_a = f_0 + \Delta f' + i\Delta f'' \quad (15)$$

The anomalous dispersion coefficients, $\Delta f'$ and $\Delta f''$, were taken from Cromer's tabulations³². In one case, this effect was used to distinguish between absolute molecular configurations³³.

(2) $T_i(S)$. The assumption is that atoms are vibrating in a harmonic potential field, either isotropically or anisotropically. The expressions used for $T_i(S)$ are;

$$T_i(S) = \exp[-\frac{1}{4}B(2 \sin \theta/\lambda)^2] \quad (16)$$

for the isotropic case where $B = 8\pi^2\bar{U}^2$, and \bar{U}^2 is the mean square amplitude of vibration. For the anisotropic case the expression used is;

$$T_i(S) = \exp[-2\pi^2(U_{11}h^2a^{*2} + U_{22}k^2b^{*2} + U_{33}l^2c^{*2} + 2U_{12}hka^*b^* + 2U_{13}hla^*c^* + 2U_{23}klb^*c^*)] \quad (17)$$

where the U_{ij} are now the thermal parameters expressed in terms of mean-square amplitudes of vibration in angstroms ~~xx~~ 2.

Structure factor and refinement calculations described in this thesis were based on F and the quantity $\sum w(|F_O| - |F_c|)^2$ was minimised. The weights w , were taken as $4F_O^2/\sigma^2(F_O^2)$. The conventional R factor, R_1 , and the weighted R factor, R_2 , are defined as:

$$R_1 = \frac{\sum ||F_O| - |F_c||}{\sum |F_O|} \quad (18)$$

$$R_2 = \left[\frac{\sum w(|F_O| - |F_c|)^2}{\sum w|F_O|^2} \right]^{\frac{1}{2}} \quad (19)$$

3.6 The Patterson Function

The Patterson function³⁴, commonly written in the form of a Fourier series;

$$P(u,v,w) = V^{-1} \sum_h \sum_k \sum_l |F(hkl)|^2 \cos 2\pi(hu + kv + lw) \quad (20)$$

shows maxima corresponding to interatomic vectors between all pairs of atoms at $(u+x, v+y, w+z)$ and (x, y, z) in the unit cell. For a structure containing N atoms per unit cell, the Patterson synthesis will show N^2 peaks, of which N will be vectors of zero length from each atom to itself. A peak corresponding to an

interatomic vector between symmetry-equivalent atoms is termed a Harker peak³⁵. These peaks are concentrated in Patterson space on Harker sections³⁶ and Harker lines. This arises from space group symmetry, in that symmetry elements like screw axes or glide planes give rise to interatomic vectors with one or two constant coordinates. These constant values are the same for all atoms in the unit cell.

3.7 Difference Fourier Synthesis

This may be expressed in the form

$$\Delta\rho(xyz) = 2V^{-1} \sum_h \sum_k \sum_l (|F_0| - |F_c|) \cdot (\cos \alpha_c \cos 2\pi\delta + \sin \alpha_c \sin 2\pi\delta) \quad (21)$$

where α_c is the phase of F_c , and $\delta = hx + ky + lz$. One of h , k or l runs from 0 to ∞ (on the assumption that Friedel's law holds) and the other two take values from $-\infty$ to ∞ . In so far as the phase of F_c is a valid approximation to the phase of F_0 a difference Fourier synthesis represents the difference in electron density between the actual structure and the model used to calculate F_c .

The function was evaluated within the unit cell at discrete sampling points arranged in a regular lattice and with uniform spacings (about 0.3Å) between points

parallel to each unit cell axis. The output from program FOURIER was usually represented as a list of interpolated peak positions with heights based on an arbitrary normalized scale. Alphameric plots and contoured maps were optional.

CHAPTER IV

Crystal Structure of

Bis(methynyltricobalt enneacarbonyl), $[\text{CCo}_3(\text{CO})_9]_2$

4.1 Experimental

The compound was prepared by Dr B.H. Robinson, University of Otago, from $\text{BrCCo}_3(\text{CO})_9$ and toluene using the method previously reported¹. Dark brown crystals of an irregular shape were obtained by recrystallisation from the solvent.

Crystallographic Data - $\text{Co}_6\text{C}_{20}\text{O}_{18}$ F.W. 881.8 is monoclinic with $a = 16.268$ (3), $b = 9.450$ (2), $c = 18.906$ (4) Å, $\beta = 106.79$ (2)°; $V = 2801$ Å³; $d_{\text{obs}} = 2.10$ (2) g cm⁻³; $d_{\text{calc}} = 2.09$ g cm⁻³; $\mu(\text{Mo-K}\alpha) = 13.5$ cm⁻¹.

Systematic absences occurred for $h k l$ reflections when $(h+k)$ was odd and for $h 0 l$ reflections when l was odd. Possible space groups were therefore $C_{2h}^6 - C 2/c$ or $C_s^4 - Cc$. The centrosymmetrical space group $C 2/c$ was indicated both by intensity statistics of the full data set and also by the distribution of peaks in a three-dimensional Patterson map and was confirmed by the subsequent successful structure solution and refinement. This space group required molecular symmetry $C_i - 1$ or $C_2 - 2$.

Unit cell dimensions and their estimated standard deviations were obtained at room temperature ($23 \pm 2^{\circ}\text{C}$) with Mo-K α_1 radiation ($\lambda = 0.7093\overset{\circ}{\text{\AA}}$) using the least-squares procedure described in Chapter II. The experimental density was determined using a calibrated density gradient column containing a mixture of bromoform and m-xylene.

Diffraction data were obtained from a crystal fragment whose shape approximated to that of a parallelepiped with boundary faces defined by the forms {001}, {010}, and {20 $\bar{1}$ }. Crystal dimensions normal to these faces were 0.15, 0.25 and 0.32 mm respectively. A preliminary mosaicity check of the crystal showed that the width at half-height of intense low-angle reflections was acceptably low at 0.10° . Intensity data were recorded as described in Chapter II. Attenuators were automatically inserted in the primary beam if the total scan count exceeded 150,000/sec. The intensities of three standard reflections were monitored throughout the data collection and showed no significant variation. The data were scaled only to allow for the different scan widths. A total number of 4087 reflections (both $h\ k\ l$ and $\bar{h}\ \bar{k}\ \bar{l}$) were collected in this way, and after averaging of equivalent forms, there was a total of 1947 independent reflections recorded within the range

$0 < 2\theta \leq 46^\circ$ of which 297 were considered unobserved as they had intensities less than $\sigma(I)$.

Absorption corrections were applied before the final refinement and the transmission factors ranged from 0.68 to 0.83 for the 002 and the 021 reflections respectively.

4.2 Solution and Refinement

The structure was solved, using the symbolic addition procedure as outlined in Chapter III. Positive signs (a phase of 0.0π) were assigned to the two reflections $\bar{4} 8 11$ and $3 7 2$ to define the origin and symbolic signs were assigned to the phases of the reflections $\bar{1} 1 13$, $\bar{10} 6 9$, $1 1 13$, and the $0 0 18$ to initiate the symbolic addition procedure. In this way a self consistent set of signs was obtained for the symbols, and phases were assigned to the 263 data having $|E| \geq 1.5$. The resulting E-map showed three predominant peaks which proved to be the sites of the three independent Co atoms. Preliminary least-squares refinement of their positional and isotropic thermal parameters yielded values for R_1 and R_2 of 0.26 and 0.33 respectively.

At this stage a novel method was used to locate the remaining atoms. For the five tricobalteneacarbonyl

derivatives whose structures had previously been determined in the laboratory the conformations of the $\text{CCo}_3(\text{CO})_9$ units were closely similar. The same relative positions of the carbon and oxygen atoms found for one of these compounds, $[\text{C}_2\text{Co}_3(\text{CO})_9]_2$, were therefore assumed. These positions were sufficiently close approximations for the refinement to proceed smoothly.

Refinement of positional and isotropic thermal parameters for all 22 atoms converged at $R_1 = 0.080$ and $R_2 = 0.090$. Further refinement with anisotropic thermal parameters for the Co atoms only (suggested by difference electron density maps) lowered R_1 and R_2 to 0.066 and 0.076 respectively. There was no evidence of pronounced thermal anisotropy of the carbonyl groups.

Examination of average values of the minimized function over ranges of $|F_0|$ and $\sin \theta/\lambda$ showed that the most intense reflections were being overweighted. The data were therefore reprocessed with an increased value of 0.07 for the parameter 'p' in the expression for $\sigma(I)$. Absorption corrections were then applied and the equivalent forms were averaged. All parameters were then refined to convergence, the maximum parameter shift on the last cycle being less than one-tenth of its estimated standard deviation.

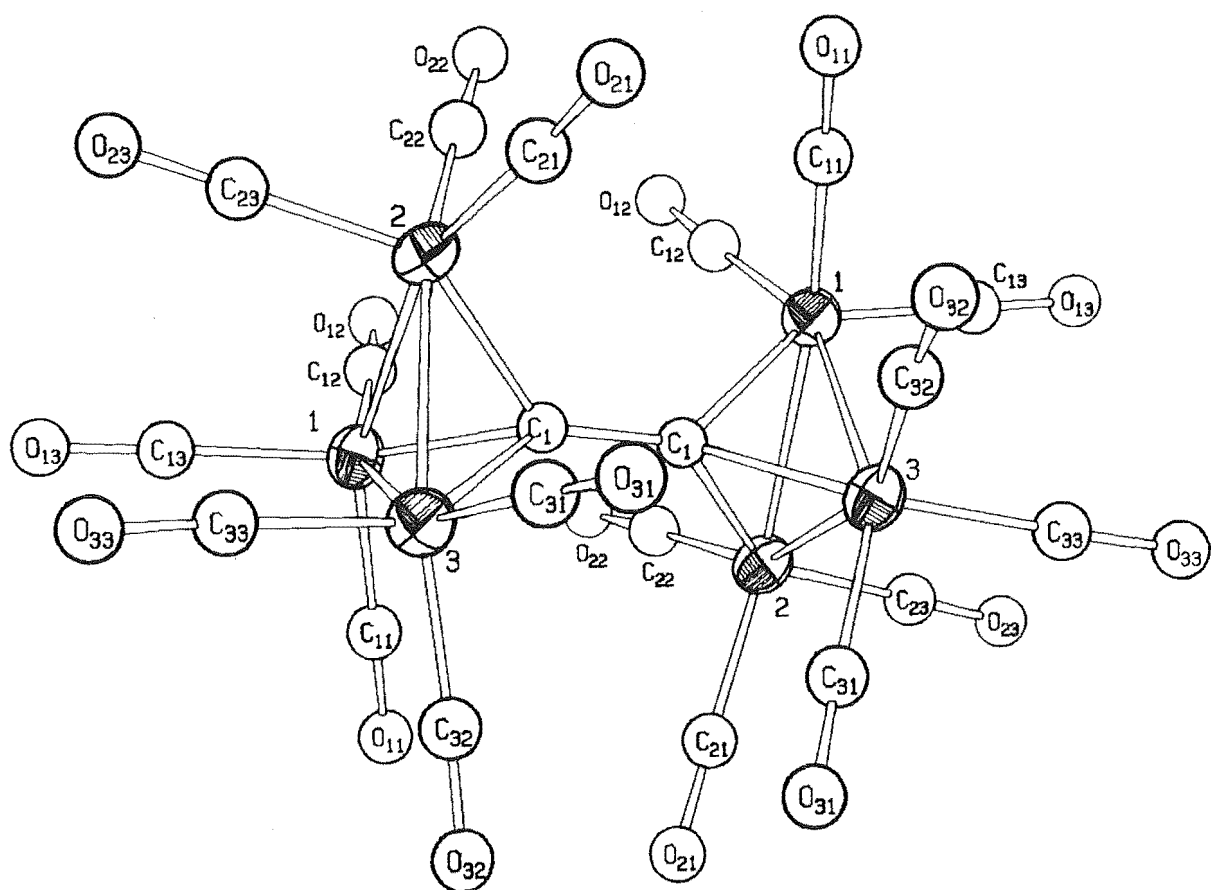


Figure 4.1 A Perspective View of $[\text{CCo}_3(\text{CO})_9]_2$

Examination of intense low angle reflections indicated that secondary extinction was appreciable. This effect was corrected for, assuming the angularly dependent extinction function derived by Zachariasen³⁷ and incorporating this into the least-squares equation as suggested by Larson³⁸. The actual function minimized at this point was $\sum w[(|F_O| - |F_c|/Z)]^2$ where Z is given by the expression

$$Z = [g\beta I + (1 + (g\beta I)^2)^{\frac{1}{2}}]^{\frac{1}{2}}$$

In this expression β is Zachariasen's polarization correction term, $(1 + \cos^4 2\theta)/(1 + \cos^2 2\theta)^2$ and the final value of the extinction parameter g was $0.4 (1) \times 10^6$.

Final positional and thermal parameters for all atoms are listed in Tables 4.1 and 4.2 and observed and calculated structure factors for all 1650 reflections used in the refinement are given in Appendix B. Examination of the 297 reflections treated as unobserved showed no anomalies of the type $|F_c| \gg |F_O|$.

4.3 Description of Structure and Discussion

The crystal structure consists of well separated molecules of $[CCO_3(CO)_9]_2$; the closest intermolecular contact is 3.07\AA . General perspective views of the whole molecule are shown in Figures 4.1 and 4.2,

TABLE 4.1

POSITIONAL AND THERMAL PARAMETERS FOR $[\text{Co}_3(\text{CO})_9]_2$

Atom	x	y	z	U_{11}^a	U_{22}	U_{33}	U_{12}	U_{13}	U_{23}
Co(1)	0.40066(6)	0.1447(1)	0.13720(5)	0.03168	0.02697	0.02774	-0.00354	0.00797	-0.00290
Co(2)	0.54594(7)	0.2099(1)	0.13718(6)	0.03318	0.02888	0.02866	0.00144	0.01446	-0.00065
Co(3)	0.44062(7)	0.3952(1)	0.13716(6)	0.03410	0.02479	0.02881	0.00271	0.00989	0.00351

Table 4.1 (contd.)

Atom	x	y	z	B(\AA^2)
C(11)	0.3060(5)	0.1738(9)	0.1651(5)	2.9(2)
C(12)	0.3528(6)	0.1228(9)	0.0403(5)	3.5(2)
C(13)	0.4148(5)	-0.038(1)	0.1620(5)	3.2(2)
C(21)	0.6424(6)	0.3117(9)	0.1618(5)	3.3(2)
C(22)	0.5925(5)	0.0406(9)	0.1649(4)	2.9(2)
C(23)	0.5318(6)	0.1966(9)	0.0402(5)	3.6(2)
C(31)	0.5161(5)	0.5359(9)	0.1656(4)	2.8(2)
C(32)	0.3544(6)	0.4764(9)	0.1625(5)	3.3(2)
C(33)	0.4061(6)	0.428(1)	0.0396(5)	3.7(2)
O(1)	0.4868(4)	0.2492(7)	0.2121(4)	1.8(2)
O(11)	0.2464(4)	0.1899(7)	0.1832(4)	4.7(1)
O(12)	0.4208(5)	-0.1563(8)	0.1754(4)	5.0(2)
O(13)	0.3217(5)	0.1106(8)	-0.0217(4)	6.1(2)
O(21)	0.7047(5)	0.3707(8)	0.1749(4)	5.1(2)
O(22)	0.6239(4)	-0.0660(8)	0.1842(4)	4.7(1)
O(23)	0.5225(5)	0.1880(9)	-0.0232(5)	6.4(2)
O(31)	0.5626(4)	0.6274(7)	0.1829(4)	4.7(1)
O(32)	0.2990(5)	0.5336(8)	0.1750(4)	5.1(2)
O(33)	0.3820(5)	0.4522(9)	-0.0232(4)	6.1(2)

^aThe dimensions of U_{ij} are \AA^2 and the expression for the atomic temperature factor is

$$\exp[-2\pi^2(h^2a^{*2}U_{11} + k^2b^{*2}U_{22} + l^2c^{*2}U_{33} + 2hka^*c^*U_{12} + 2hla^*c^*U_{13} + 2klb^*c^*U_{23})].$$

TABLE 4.2

Root-Mean-Square Amplitudes of Vibration (\AA)

Atom	Minimum	Intermediate	Maximum
Co(1)	0.154(2)	0.171(2)	0.183(2)
Co(2)	0.149(2)	0.171(2)	0.189(2)
Co(3)	0.151(2)	0.172(2)	0.187(2)

TABLE 4.3
Bond Distances (Å) ^a

Co(1)-Co(2)	2.457(2)	Co(1)-C(1)	1.95(1)
Co(1)-Co(3)	2.456(2)	Co(2)-C(1)	1.97(1)
Co(2)-Co(3)	<u>2.457(1)</u>	Co(3)-C(1)	<u>1.97(1)</u>
	2.457(1)		1.96(1)
Co(1)-O(11)	1.80(1)	C(11)-O(11)	1.13(1)
Co(1)-O(12)	1.78(1)	C(12)-O(12)	1.14(1)
Co(1)-O(13)	1.78(1)	C(13)-O(13)	1.15(1)
Co(2)-O(21)	1.79(1)	C(21)-O(21)	1.12(1)
Co(2)-O(22)	1.78(1)	C(22)-O(22)	1.14(1)
Co(2)-O(23)	1.79(1)	C(23)-O(23)	1.15(1)
Co(3)-O(31)	1.79(1)	C(31)-O(31)	1.13(1)
Co(3)-O(32)	1.79(1)	C(32)-O(32)	1.14(1)
Co(3)-O(33)	<u>1.79(1)</u>	C(33)-O(33)	<u>1.15(1)</u>
	1.79(1)		1.14(1)
C(1)-C(1')	1.37(1)		

^aThe figures in parentheses are e.s.d.'s in the last significant figure. Mean values are calculated using the expression

$$\bar{l} = \Sigma(l_i/\sigma_i^2)/\Sigma(1/\sigma_i^2)$$

The e.s.d. of the mean value is calculated as a root mean square deviation using the expression

$$\sigma(\bar{l}) = [\Sigma(l-l_i)^2/(N-1)]^{1/2}$$

TABLE 4.4

Bond Angles (Degrees) ^a

C(1)-Co(1)-Co(2)	51.5(2)	Co(1)-Co(2)-C(23)	98.3(3)
C(1)-Co(1)-Co(3)	51.4(2)	Co(1)-Co(3)-C(33)	99.4(3)
C(1)-Co(2)-Co(3)	51.3(2)	Co(2)-Co(3)-C(33)	97.9(3)
C(1)-Co(2)-Co(1)	50.9(2)	Co(2)-Co(1)-C(13)	99.6(3)
C(1)-Co(3)-Co(1)	51.0(2)	Co(3)-Co(1)-C(13)	98.6(3)
C(1)-Co(3)-Co(2)	<u>51.4(2)</u>	Co(3)-Co(2)-C(23)	<u>99.6(3)</u>
	51.3		98.9
C(1)-Co(1)-C(11)	102.3(3)	Co(1)-Co(2)-C(22)	96.1(3)
C(1)-Co(1)-C(12)	106.6(3)	Co(1)-Co(3)-C(32)	100.5(3)
C(1)-Co(2)-C(21)	107.0(3)	Co(2)-Co(3)-C(31)	96.1(3)
C(1)-Co(2)-C(22)	102.4(3)	Co(2)-Co(1)-C(12)	101.0(3)
C(1)-Co(3)-C(31)	102.5(3)	Co(3)-Co(1)-C(11)	96.0(3)
C(1)-Co(3)-C(32)	<u>106.1(3)</u>	Co(3)-Co(2)-C(21)	<u>100.6(3)</u>
	106.6		98.4
C(11)-Co(1)-C(13)	99.1(4)	Co(1)-Co(2)-C(21)	156.3(3)
C(12)-Co(1)-C(13)	98.2(4)	Co(1)-Co(3)-C(31)	151.3(3)
C(21)-Co(2)-C(23)	98.4(4)	Co(2)-Co(3)-C(32)	156.0(3)
C(22)-Co(2)-C(23)	99.0(4)	Co(2)-Co(1)-C(11)	151.5(3)
C(31)-Co(3)-C(33)	99.4(4)	Co(3)-Co(1)-C(12)	156.5(3)
C(32)-Co(3)-C(33)	<u>99.3(4)</u>	Co(3)-Co(2)-C(22)	<u>151.5(3)</u>
	98.9		153.8

Table 4.4 (contd.)

Co(1)-Co(2)-Co(3)	60.0(1)	C(11)-Co(1)-C(12)	97.4(4)
Co(2)-Co(3)-Co(1)	60.0(1)	C(21)-Co(2)-C(22)	97.8(4)
Co(3)-Co(1)-Co(2)	<u>60.0(1)</u>	C(31)-Co(3)-C(32)	<u>97.5(4)</u>
	60.0		97.6
C(1')-C(1)-Co(1)	134.5(4)	Co(1)-C(11)-O(11)	178.7(8)
C(1')-C(1)-Co(2)	133.8(4)	Co(1)-C(12)-O(12)	177.0(8)
C(1')-C(1)-Co(3)	<u>132.9(4)</u>	Co(1)-C(13)-O(13)	179.1(8)
	133.7	Co(2)-C(21)-O(21)	176.2(8)
		Co(2)-C(22)-O(22)	178.1(8)
C(1)-Co(1)-C(13)	144.5(4)	Co(2)-C(23)-O(23)	179.9(8)
C(1)-Co(2)-C(23)	143.9(4)	Co(3)-C(31)-O(31)	178.5(8)
C(1)-Co(3)-C(33)	<u>143.6(4)</u>	Co(3)-C(32)-O(32)	175.7(8)
	144.0	Co(3)-C(33)-O(33)	<u>178.0(8)</u>
			177.9
Co(1)-C(1)-Co(2)	77.6(2)		
Co(1)-C(1)-Co(3)	77.6(2)		
Co(2)-C(1)-Co(3)	<u>77.3(2)</u>		
	77.5		

^a See footnote to Table 4.3. RMS deviations are not given for mean values of angles assumed to be chemically equivalent because these usually far exceed the esd's of individual values.

TABLE 4.5

SELECTED INTRAMOLECULAR NON-BONDED DISTANCES (Å) ^a

Those within one asymmetric unit

C(11) ... C(12)	2.69	C(31) ... C(32)	2.69
C(11) ... C(13)	2.73	C(31) ... C(33)	2.74
C(12) ... C(13)	2.70	C(32) ... C(33)	2.73
C(21) ... C(22)	2.70	C(11) ... C(32)	2.98
C(21) ... C(23)	2.71	C(12) ... C(22)	2.99
C(22) ... C(23)	2.72	C(21) ... C(31)	2.99
C(13) ... C(23)	3.01		
C(13) ... C(33)	3.02		
C(23) ... C(33)	3.00		

Table 4.5 (contd.)

Those between the two parts of the dimer

	observed	calculated assum- ing molecular mirror plane	calculated assum- ing molecular centre of symmetry
O(11) ... O(21')	3.09	*	2.64
O(21) ... O(22')	3.08	*	3.39
O(31) ... O(32')	3.10	*	*
O(11) ... O(11')	*	2.42	*
O(12) ... O(12')	*	2.70	*
O(21) ... O(21')	*	2.72	*
O(22) ... O(22')	*	2.38	*
O(31) ... O(31')	*	2.42	*
O(32) ... O(32')	*	2.72	*
O(12) ... O(31')	*	*	2.63
O(22) ... O(32')	*	*	2.61

^a Distances over 3.5 Å are indicated by an asterisk.

TABLE 4.6

CARBON-CARBON BOND LENGTHS INVOLVING THE BRIDGING

CARBON ATOM IN DERIVATIVES OF $\text{YCo}_3(\text{CO})_9$

	$\text{Co}_3\text{C-C}$	$\text{Co}_3\text{C-C}$ Co	$\text{Co}_3\text{C-C}$	$\text{Co}_3\text{C-CH}_3$	
	$[\text{Co}_3(\text{CO})_9\text{C}_2]_2^a$	$\text{Co}_5(\text{CO})_{15}\text{C}_3\text{H}^b$	$\text{C}_6\text{H}_5\text{CCo}_3(\text{CO})_6^c$	$\text{CH}_3\text{CCo}_3(\text{CO})_9^d$	
	1.37(1)	1.46(2)	1.48(2)	1.53(3)	
	$\text{Co}_8(\text{CO}_{24})\text{C}_6^e$	$\text{Co}_8(\text{CO})_{24}\text{C}_6^e$	$\text{C}_6\text{H}_5\text{CCo}_3(\text{CO})_6^c$	$\text{CH}_3\text{CCo}_3(\text{CO})_8\text{P}(\text{C}_6\text{H}_5)_3^f$	
	1.36(3)	1.44(3)	1.47(3)	1.50(2)	
	$[\text{Co}_3(\text{CO})_9\text{C}]_2$				
	1.37(1)				
Average	1.37	1.45	1.48	1.51	
Reference ^g	1.37	1.45	1.45	1.46	
	$\text{C}_{\text{sp}} - \text{C}_{\text{sp}}$	$\text{C}_{\text{sp}} - \text{C}_{\text{sp}2}$	$\text{C}_{\text{sp}} - \text{C}_{\text{sp}2}$	$\text{C}_{\text{sp}} - \text{C}_{\text{sp}3}$	
a.	Reference 4	b.	Reference 7	c.	Reference 39
d.	Reference 2	e.	Reference 5	f.	Reference 40
g.	Reference 38				

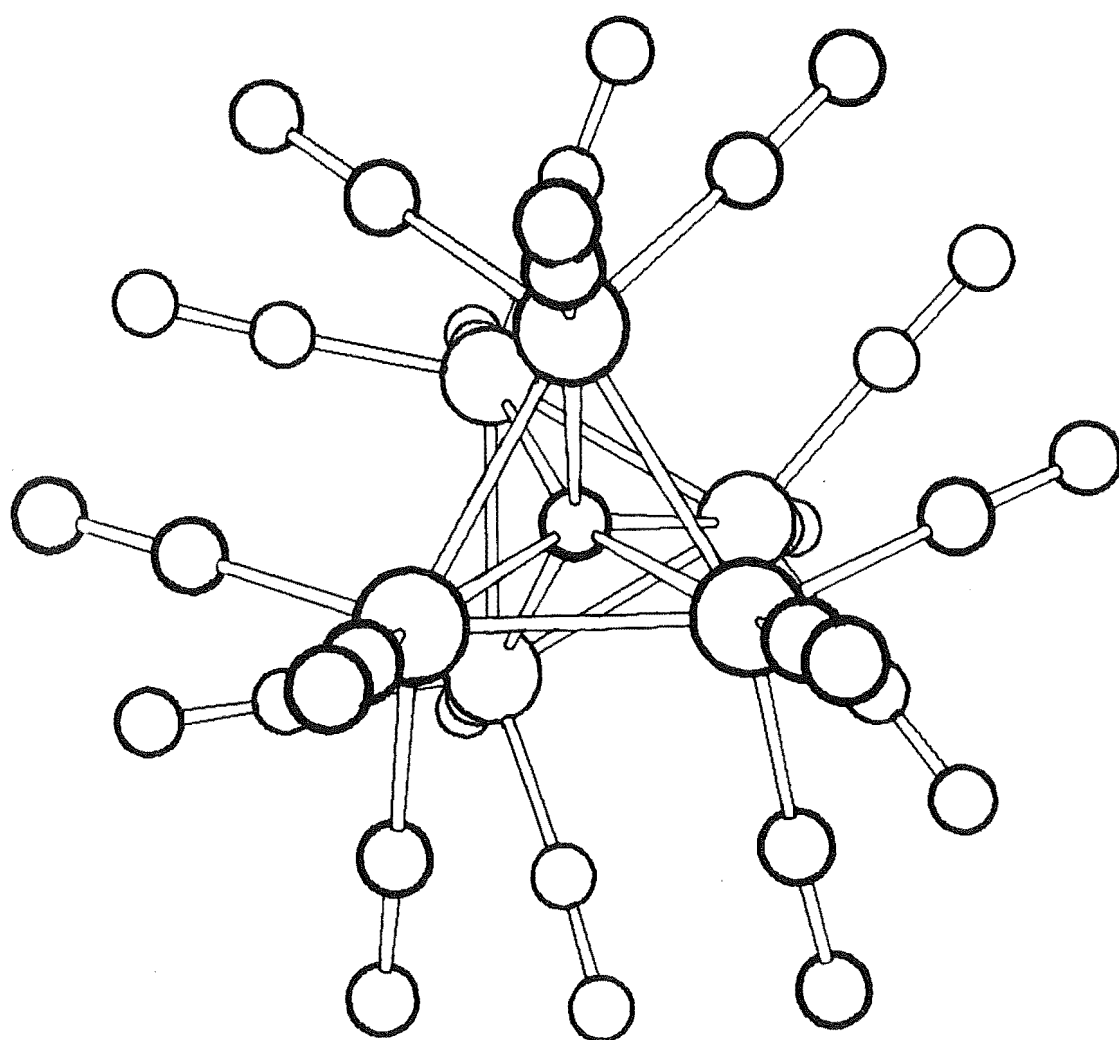


Figure 4.2 One Molecule of $[\text{CCo}_3(\text{CO})_9]_2$ viewed normal to the Co_3 triangle

indicating the numbering system used. Figure 4.3 is a stereoscopic view of the molecule. Bond lengths and angles are listed in Tables 4.3 and 4.4 respectively and Table 4.5 contains selected intramolecular non-bonded distances, both as observed and also as calculated for two hypothetical molecules of higher symmetry.

The molecule consists of two $\text{CCo}_3(\text{CO})_9$ units linked by direct bonding of the bridging carbon atoms, the crystallographic diad axis bisecting the central carbon-carbon bond so formed. The two Co_3 triangles are neither fully staggered as in the centrosymmetric $[\text{C}_2\text{Co}_3(\text{CO})_9]_2$ ⁴ nor eclipsed, so that the potential $\underline{\text{D}}_{3d}$ or $\underline{\text{D}}_{3h}$ symmetry of the whole molecule is reduced in fact to an idealised $\underline{\text{D}}_3 - \bar{3}_2$. The departures from the idealised state are, however, quite small and each unit retains its idealised $\underline{\text{C}}_{3v} - \bar{3}_m$ symmetry. As may be deduced from Figures 4.1 and 4.2, the twisting of the rigid $\text{CCo}_3(\text{CO})_9$ units about their connecting bond is such as to minimise non-bonded repulsions between carbonyl groups. This is illustrated quantitatively in Table 4.5 where actual non-bonded distances between CO groups from the two parts of the dimer are compared with those that would apply if the dimer were either eclipsed or fully staggered but with the dimensions of each

$\text{CCo}_3(\text{CO})_9$ unit unchanged. Although the CO non-bonded repulsions have been minimised by the angle of twist, a further bending of the Co-CO bonds has been required. Thus the dihedral angles between the Co_3 triangle and the planes formed by each Co atom and its associated equatorial groups have an average value of only 24.0° compared with the value of 28° in $[\text{C}_2\text{Co}_3(\text{CO})_9]_2$ ⁴, 29° in $\text{CH}_3\text{CCo}_3(\text{CO})_9$ ², and 32° in $\text{Co}_3(\text{CO})_{10}\text{BH}_2\text{N}(\text{C}_2\text{H}_5)_3$ ³⁹ in all of which compounds no such non-bonded repulsions may occur.

The bond lengths and angles of the individual units are with one exception in good agreement with those in other compounds containing similar units. The exception is the set of Co-C (bridge) bonds whose average value of $1.96(1)\text{\AA}$ observed here compared with an average value of 1.915\AA (range $1.90 - 1.92\text{\AA}$) observed for seven other compounds, and this must be considered a significant difference. This indication of a weakening of the Co-C bonds is supported by the fact that these bonds are much more easily ruptured by electron impact in the mass spectrometer than those of say $\text{Co}_5(\text{CO})_{15}\text{C}_3\text{H}$ ⁴⁰.

Of greatest importance, however, in the molecular structure is the central formally single C-C bond of length $1.37(1)\text{\AA}$. In all cases where CCo_3 units are

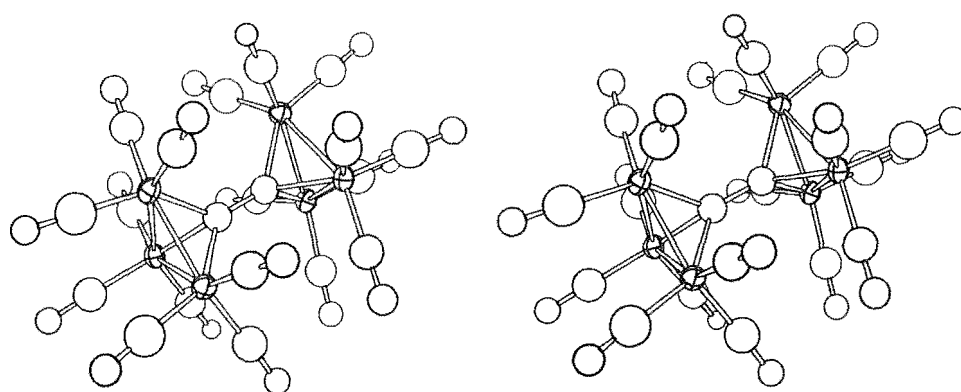


Figure 4.3 A Stereoscopic View of $[CCo_3(CO)_9]_2$

linked through a conjugated carbon chain, there is a marked shortening of the C-C bond formed by the bridging carbon atom relative to that expected of an sp^3 hybridised carbon forming a single bond. In this case, however, where there is no intervening carbon chain, the bond is in isolation and it was hoped to reach firmer conclusions as to its nature and hence, the nature of the Co-C bridging bonds themselves. Carbon-carbon single bonds as short as $1.371(5)^{\circ}\text{\AA}$ have previously been reported only in such molecules as diacetylene⁴¹ where both atoms concerned are formally sp hybridised. It is therefore assumed that the p character of the outwardly directed orbitals of the bridging carbon atoms have been reduced approximately to this level. Making the same assumption for the other compounds containing linked CCo_3 units it is found that there is excellent agreement between the observed bond lengths and those calculated for single bonds (see Table 4.6). The agreement is less good where the bridging carbon is bonded directly to a terminal group, but is still within limits of error.

It appears that the outwardly directed orbital used by the bridging carbon atom in forming a sigma bond is much reduced in character relative to sp^3 . The bridging carbon is left with 3 electrons in predominantly p orbitals available for bonding to the three cobalt atoms.

CHAPTER V

Crystal Structure of $C_{10}O_2H_{20}$

5.1 Experimental

Colourless well-formed crystals of 4-t-butyl cyclohexane-1,2-diol were obtained by recrystallisation from pentane, using a sample supplied by Dr G.R. Little.

Crystallographic Data: $C_{10}O_2H_{20}$, F.W. 172.3 is triclinic with $a = 12.268$ (3), $b = 15.921$ (3), $c = 6.332$ (1) Å, $\alpha = 82.5$ (2), $\beta = 114.45$ (6), $\gamma = 111.13$ (6)°; $V = 1049.9$ Å³; $Z = 4$; $d_{calc} = 1.90$ g cm⁻³; $\mu(Cu-K\alpha) = 5.87$ cm⁻¹. Possible space groups are $C_1^1 - P 1$ or $C_1^1 - P \bar{1}$. The centrosymmetric space group $P \bar{1}$ was assumed and this was confirmed by the subsequent successful structure solution and refinement. The reduced cell has the dimensions: $a = 11.238$, $b = 15.921$, $c = 6.332$ Å, $\alpha = 97.5$, $\beta = 96.42$, $\gamma = 108.68$ °, and is related to the cell used in this analysis by the transformation matrix α ;

$$\alpha = \begin{vmatrix} 1 & 0 & 1 \\ 0 & 1 & 0 \\ 0 & 0 & \bar{1} \end{vmatrix}.$$

Unit cell and crystal orientation parameters were obtained at room temperature ($23 \pm 2^\circ\text{C}$) with Cu-K α radiation ($\lambda = 1.4518$ Å) using the least-squares

procedure described in Chapter II. Diffraction data were obtained from a crystal with faces defined by the forms $\{010\}$, $\{\bar{1}10\}$, and $\{11\bar{1}\}$, and dimensions normal to these faces of 0.15, 0.075, and 0.45 mm respectively. A preliminary check of the mosaicity of the crystal gave acceptably low values of 0.1° .

Data were collected using scans of 0.8° and 1.2° in 2θ composed of 40 and 60 equal steps of one second duration for the ranges $2\theta \leq 70^\circ$ and $70^\circ < 2\theta \leq 88^\circ$ respectively. The intensities of 2479 reflections (made up from the Friedel equivalent reflections $h k l$ and $\bar{h} \bar{k} \bar{l}$) were recorded and after averaging these equivalent forms the data set consisted of 1612 independent observations of which 1199 had their intensity I greater than the standard error $\sigma(I)$. The factor p in the expression for $\sigma(I)$ was assigned a value of 0.075. Absorption corrections were applied and transmission factors ranged from 0.897 to 0.959 for the $\bar{4} 3 5$ and $0 \bar{1} \bar{1}$ reflections respectively.

5.2 Structure Solution and Refinement

Two different methods were employed in attempts to solve this structure before a correct solution was obtained. These were the symbolic addition procedure and the use of Patterson superposition techniques.

The first applications of the symbolic addition procedure were unsuccessful. To assign symbolic phases to those data having $|E| \geq 1.7$, four symbols were required. Past experience has shown that for the triclinic case, the determination of absolute signs for symbols is very difficult. Thus it was necessary to evaluate fifteen Fourier syntheses obtained from the permutations of the signs for the four symbols. Karle and Karle²⁰ have suggested that when calculating an E-map the ideal number of input data should be ten times the number of non-hydrogen atoms in the asymmetric unit. To achieve this number phases had to be determined for those data having $|E| \geq 1.3$, approximately 230 in number.

The resultant Fourier syntheses did not reveal a chemically reasonable structure. Some had large peaks at, or close to, the origin, which was generally indicative of an incorrect solution. Any map which had a large disparity of peak heights was assumed not to contain a true image of the structure. Fragments were indicated in some cases, but in no case permitted development of a complete structure. The main problems with this approach were an inability to determine the 'correctness' (internal consistency) of a particular sign set.

Other attempts were made to solve the structure, using Patterson superposition techniques⁴⁴. It was hoped that an image of the structure could be readily extracted from the three-dimensional Patterson synthesis by superposition upon either a rear-origin multiple weight vector or a suspected Harker vector. Both types of vectors were used as starting points for multiple and single superpositions but the difficulty of extracting images from the resultant maps was a major problem.

Prior to calculation of the Patterson map the coefficients in the Fourier series (expression (20) in Chapter III) were modified to those which would have been obtained if the diffraction centres were point atoms at rest. This process of sharpening involved modification of $F(h\ k\ l)$ such that dependence of the scattering factors on $\sin \theta/\lambda$, and the effects of thermal vibration are removed. The large origin peak was also partially removed. An overall temperature factor and scale factor were obtained, as described in Chapter III, and the sharpened coefficients were obtained using the expression:

$$|F_s(h\ k\ l)|^2 = K^2 |F(h\ k\ l)|^2 \exp(2B\lambda^{-2} \sin^2 \theta) \\ \frac{\sum_N Z^2}{\sum f^2} - x \frac{\sum_N Z^2}{\sum f^2}.$$

where the second term removes a fraction x of the origin peak.

The superposition maps produced contained numerous peaks which were very 'sharp' but at best only partial images were extracted. The results were not conclusive. After the structure had been successfully solved, the Patterson map was examined. A superposition was carried out using one of these vectors as a starting point. Atomic positions could be ascribed to peaks on the resultant map, but these peaks were indistinguishable from many others in the map. It would have been a very difficult task to extract a true image from this map.

A correct solution of the structure was finally achieved using a combined application of the symbolic addition procedure and the tangent formula. The origin was specified by assigning positive signs (a phase of 0.0 radians) to three reflections ($\bar{2}$ 0 1, $\bar{8}$ 3 3, and $\bar{5}$ 5 1), and to initiate the symbolic addition procedure the signs of four reflections ($\bar{2}$ 2 0, 0 6 4, 2 4 $\bar{5}$ and $\bar{3}$ 1 1) were represented by symbols. Symbolic signs were determined for the 120 data having $E > 1.7$ and thus there were 15 possible E-maps to calculate, excluding the case where all symbols have positive signs.

To obtain a measure of the 'correctness' of a sign set and to reliably extend this sign set (i.e. to increase the number of phased data to include those with $1.7 > |E| \geq 1.3$) the tangent formula was used, as described in Chapter III. The value for R-Karle, as defined in Chapter III, was used as a guide to indicate which sign set would most probably reveal the structure. It was found that the tangent refinement which gave the lowest value for the R-Karle, had correctly phased the 238 data having $|E| \geq 1.3$. The Fourier synthesis calculated with these signed $|E|$ values as coefficients revealed all but one of the non-hydrogen atoms in the asymmetric unit.

Preliminary refinement gave values for R_1 and R_2 of 0.288 and 0.364 respectively. No corrections were made for anomalous scattering. The last non-hydrogen atom was located from a difference Fourier synthesis and the isotropic model converged with values for R_1 and R_2 of 0.128 and 0.169 respectively. Before the refinement procedure was continued the positions of all 40 independent hydrogen atoms were determined. Of these, 18 were in readily calculable positions (assuming tetrahedral geometry of the ring atoms). Peaks were found, by difference Fourier techniques, which were very close to all such calculated positions.

Another 18 of the hydrogen atoms were from methyl groups and their positions were determined by matching sets of three peaks from the Fourier maps to idealised tetrahedral geometry around each methyl carbon atom. The last hydrogen atoms to be located were those bonded to the oxygen atoms. Their positions were determined from a series of difference Fourier syntheses calculated with decreasing shells of data defined by a maximum $\sin \theta$ value. Those peaks attributed to hydrogen atoms stayed consistently well above the noise level of the difference maps.

The refinement continued with all hydrogen atoms included in fixed positions, with fixed isotropic temperature factors of 9.0\AA^2 , and with anisotropic thermal parameters ascribed to the oxygen atoms and the t-butyl group atoms. This step was taken to account for their consistently higher isotropic thermal parameters. The converged values for R_1 and R_2 were 0.063 and 0.068. Shifts in the last cycle of refinement were all less than one tenth their estimated standard deviations. A final difference Fourier synthesis revealed peaks whose heights were one half the height of the last hydrogen atoms which were located by this technique. The weighting scheme appeared to be satisfactory in that the minimised function showed no

systematic dependence upon $|F_0|$ or $\sin \theta/\lambda$. A structure factor calculation using the data considered to be unobserved revealed no anomalies of the type $|F_c| \gg |F_0|$. There was no evidence of secondary extinction amongst the intense low angle reflections and no correction was applied.

The positional and thermal parameters obtained from the final cycle of least-squares refinement are listed in Table 5.1 together with the assigned positions for all hydrogen atoms.

Derived root-mean-square amplitudes of vibration for the anisotropic atoms are listed in Table 5.2. A listing of the final values of F_0 and F_c is given in Appendix B.

Subsequent to this refinement, interest was aroused in the extent and type of hydrogen bonding in this crystal structure. Consequently, the positional and thermal parameters of these hydrogen atoms involved were refined along with the rest of the structure. The results were inconclusive in that the overall agreement was improved, but the errors in the positional parameters of the hydrogen atoms precluded any detailed analysis of the hydrogen bonding. The final values for R_1 and R_2 after this refinement were 0.050 and 0.062, respectively.

5.3 Description of Structure and Discussion

The crystal structure determination has established that the molecules of 4-t-butyl-cyclohexane-1,2-diol are, as expected, the 1 β , 2 β -isomer, with the cyclohexane ring in the chair conformation. A summary of the intramolecular bonding distances and angles is given in Tables 5.3 and 5.4. Figures 5.1 and 5.2 show the atom labelling within the two independent molecules in the asymmetric unit. Figure 5.3 shows the contents of two unit cells and illustrates the extensive inter-molecular hydrogen bonding found in this crystal structure.

The molecular dimensions of this diol do not vary greatly from those previously reported for similar compounds. The endocyclic C-C distances in the two cyclohexane rings have mean values of 1.53(1) and 1.53 (1) $\overset{\circ}{\text{\AA}}$ respectively, which compare favourably with those found for myo-inositol⁴⁵ (1.52 $\overset{\circ}{\text{\AA}}$), epi-inositol⁴⁶ (1.53 $\overset{\circ}{\text{\AA}}$), cyclohexane-1,1-diacetic acid⁴⁷ (1.54 $\overset{\circ}{\text{\AA}}$), and cyclo-hexyl-amine hydrochloride⁴⁸ (1.52 $\overset{\circ}{\text{\AA}}$). The C-C bond distances within the t-butyl groups average to 1.53 (1) $\overset{\circ}{\text{\AA}}$ for the two independent molecules, and the average value for the exocyclic bonds joining the t-butyl groups to the cyclohexane rings is 1.55 (1) $\overset{\circ}{\text{\AA}}$.

TABLE 5.1
POSITIONAL AND THERMAL PARAMETERS^a FOR C₁₀O₂H₂₀

Atom	x	y	z	U ₁₁	U ₂₂	U ₃₃	U ₁₂	U ₁₃	U ₂₃
O(10)	0.4089(3)	0.0573(2)	0.7403(6)	0.07403	0.03576	0.05677	0.01546	0.01893	-0.00338
O(11)	0.5170(3)	0.0900(2)	0.2230(6)	0.05691	0.03960	0.05371	0.01252	0.02103	0.00194
O(20)	0.2813(3)	0.0577(2)	0.2640(6)	0.01683	0.05122	0.06290	0.00875	0.01878	-0.01232
O(21)	0.3098(3)	-0.1134(2)	0.2935(6)	0.05892	0.07553	0.06662	0.03218	0.02403	0.00441
C(16)	0.6370(5)	0.3860(3)	0.295(1)	0.06508	0.03619	0.06971	0.00910	0.02928	-0.00130
C(17)	0.5498(6)	0.4278(4)	0.316(1)	0.09163	0.06649	0.11302	0.03090	0.03618	-0.02375
C(18)	0.7346(6)	0.3802(4)	0.537(1)	0.10673	0.07230	0.06991	0.02551	0.00220	-0.02236
C(19)	0.7126(6)	0.4508(4)	0.158(1)	0.09460	0.04829	0.11445	-0.00198	0.05520	-0.00767
C(26)	-0.0652(5)	-0.2916(4)	-0.170(1)	0.05370	0.04863	0.06122	0.00375	0.01921	-0.00353
C(27)	-0.0957(6)	-0.3013(4)	-0.429(1)	0.10413	0.07710	0.07524	-0.00465	0.03180	-0.01949
C(28)	-0.0286(6)	-0.3724(4)	-0.048(1)	0.09088	0.04884	0.10564	0.00911	0.02634	-0.00117
C(29)	-0.1863(6)	-0.2957(4)	-0.150(1)	0.05169	0.10519	0.09373	-0.00433	0.02719	-0.01153

Table 5.1 (contd.)

Atom	x	y	z	B(\AA^2)	Atom	x	y	z	B(\AA^2)
C(10)	0.4775(5)	0.1477(3)	0.8303(9)	4.1(1)	C(20)	0.1740(5)	-0.0225(4)	0.1664(9)	4.4(1)
C(11)	0.5750(5)	0.1454(3)	0.0715(9)	3.9(1)	C(21)	0.1981(5)	-0.1055(3)	0.2986(9)	4.2(1)
C(12)	0.6493(4)	0.2415(3)	0.1756(8)	4.2(1)	C(22)	0.0818(5)	-0.1895(3)	0.1907(9)	4.4(1)
C(13)	0.5632(5)	0.2912(3)	0.1771(9)	4.1(1)	C(23)	0.0468(5)	-0.2027(3)	-0.0677(9)	4.2(1)
C(14)	0.4653(5)	0.2908(3)	0.9304(9)	4.5(1)	C(24)	0.0245(5)	-0.1183(4)	-0.1960(9)	4.9(1)
C(15)	0.3888(5)	0.1943(3)	0.8268(9)	4.6(1)	C(25)	0.1407(5)	-0.0323(4)	-0.0896(9)	5.1(1)

Table 5.1 (contd.)

Atom	x	y	z	Atom	x	y	z
H(101)	0.523	0.182	0.728	H(201)	0.104	-0.013	0.190
H(111)	0.637	0.119	0.067	H(211)	0.215	-0.099	0.464
H(121)	0.710	0.238	0.338	H(221)	0.100	-0.242	0.277
H(122)	0.699	0.276	0.080	H(222)	0.008	-0.181	0.208
H(131)	0.517	0.259	0.276	H(231)	0.116	-0.214	-0.089
H(141)	0.405	0.320	0.927	H(241)	0.010	-0.124	-0.362
H(142)	0.511	0.327	0.827	H(242)	-0.051	-0.111	-0.187
H(151)	0.341	0.160	0.923	H(251)	0.120	0.020	-0.172
H(152)	0.328	0.197	0.664	H(252)	0.215	-0.038	-0.110
H(171)	0.488	0.439	0.154	H(271)	-0.167	-0.358	-0.505
H(172)	0.593	0.484	0.408	H(272)	-0.017	-0.301	-0.446
H(173)	0.490	0.382	0.388	H(273)	-0.117	-0.247	-0.514
H(181)	0.695	0.330	0.631	H(281)	-0.098	-0.434	-0.116
H(182)	0.777	0.437	0.635	H(282)	-0.015	-0.374	0.125
H(183)	0.807	0.362	0.535	H(283)	0.052	-0.373	-0.050
H(191)	0.777	0.426	0.147	H(291)	-0.177	-0.293	0.014
H(192)	0.763	0.514	0.231	H(292)	-0.262	-0.354	-0.225
H(193)	0.656	0.458	0.992	H(293)	-0.217	-0.245	-0.238
H(10)	0.351	0.069	0.510	H(20)	0.367	0.053	0.197
H(11)	0.510	0.013	0.204	H(21)	0.390	-0.135	0.502

^aThe temperature factor expression for the anisotropic atoms is

$$\exp[-2\pi^2(U_{11}h^2a^{*2} + U_{22}k^2b^{*2} + U_{33}l^2c^{*2} + 2U_{12}hka^*b^*$$

$$+ 2U_{13}hla^*c^* + 2U_{23}klb^*c^*)]$$

TABLE 5.2

ROOT MEAN SQUARE AMPLITUDES OF VIBRATION (\AA)

<u>Atom</u>	<u>Min.</u>	<u>Int.</u>	<u>Max.</u>
O(10)	0.186(6)	0.240(6)	0.290(5)
O(20)	0.205(6)	0.268(5)	0.272(5)
O(11)	0.199(5)	0.232(5)	0.249(5)
O(21)	0.223(5)	0.260(5)	0.278(5)
C(16)	0.19(1)	0.26(1)	0.27(1)
C(17)	0.21(1)	0.30(1)	0.36(1)
C(18)	0.22(1)	0.29(1)	0.39(1)
C(19)	0.21(1)	0.30(1)	0.36(1)
C(26)	0.20(1)	0.25(1)	0.27(1)
C(27)	0.23(1)	0.29(1)	0.39(1)
C(28)	0.22(1)	0.31(1)	0.36(1)
C(29)	0.21(1)	0.31(1)	0.37(1)

TABLE 5.3

BOND DISTANCES (Å) FOR THE TWO INDEPENDENT MOLECULES ^a

	n = 1	n = 2
C(n0) - O(n0)	1.431(5)	1.437(5)
C(n1) - O(n1)	1.448(6)	1.435(5)
C(n0) - C(n1)	1.508(6)	1.525(6)
C(n1) - C(n2)	1.537(6)	1.532(6)
C(n2) - C(n3)	1.536(6)	1.533(7)
C(n3) - C(n4)	1.526(7)	1.530(7)
C(n4) - C(n5)	1.543(6)	1.549(6)
C(n5) - C(n0)	1.514(6)	1.514(7)
mean	1.53(1)	1.53(1)
C(n3) - C(n6)	1.553(6)	1.552(6)
C(n6) - C(n7)	1.536(7)	1.541(7)
C(n6) - C(n8)	1.508(7)	1.524(7)
C(n6) - C(n9)	1.539(7)	1.521(7)
mean	1.53(2)	1.53(1)

^aThe figures in parentheses are e.s.d.'s in the last significant figure. Mean values are calculated using the expression

$$\bar{l} = \sum(l_i/\sigma_i^2)/\sum(1/\sigma_i^2)$$

The e.s.d. of the mean value is calculated as a root-mean-square deviation using the expression

$$\sigma(\bar{l}) = [\sum(\bar{l} - l_i)^2/(N - 1)]^{1/2}$$

TABLE 5.4

BOND ANGLES (DEGREES) FOR THE TWO INDEPENDENT MOLECULES ^a

	n = 1	n = 2
O(n0) - C(n0) - C(n1)	108.5(4)	111.1(4)
O(n0) - C(n0) - C(n5)	111.5(4)	110.8(4)
O(n1) - C(n1) - C(n2)	109.3(4)	110.9(4)
O(n1) - C(n1) - C(n0)	111.8(4)	109.6(4)
mean	110.3	110.6
C(n0) - C(n1) - C(n2)	110.0(4)	109.7(4)
C(n1) - C(n2) - C(n3)	113.2(4)	112.9(4)
C(n2) - C(n3) - C(n4)	108.7(4)	108.9(4)
C(n3) - C(n4) - C(n5)	111.8(4)	111.7(4)
C(n4) - C(n5) - C(n0)	110.5(4)	111.0(5)
C(n5) - C(n0) - C(n1)	111.9(4)	111.6(5)
mean	111.0	111.0

Table 5.4 (contd.)

	n = 1	n = 2
C(n6) - C(n3) - C(n2)	112.5(4)	112.2(5)
C(n6) - C(n3) - C(n4)	114.5(4)	114.1(4)
C(n3) - C(n6) - C(n7)	110.1(4)	109.8(5)
C(n3) - C(n6) - C(n8)	110.9(4)	110.3(5)
C(n3) - C(n6) - C(n9)	112.2(5)	112.9(5)
mean	111.1	111.0
C(n7) - C(n6) - C(n8)	107.4(5)	107.4(5)
C(n7) - C(n6) - C(n9)	107.7(5)	107.6(5)
C(n8) - C(n6) - C(n9)	108.4(5)	108.7(5)
mean	107.8	107.9

^a As for Table 5.3 but e.s.d.'s for mean values are not quoted as these usually far exceed the e.s.d.'s of the individual values.

TABLE 5.5

TORSION ANGLES (DEGREES) FOR THE TWO INDEPENDENT MOLECULES

	n = 1	n = 2
C(n0) - C(n1) - C(n2) - C(n3)	-55.4	-57.2
C(n1) - C(n2) - C(n3) - C(n4)	55.1	56.5
C(n2) - C(n3) - C(n4) - C(n5)	-55.4	-55.0
C(n3) - C(n4) - C(n5) - C(n0)	57.0	55.8
C(n4) - C(n5) - C(n0) - C(n1)	-56.5	-55.7
C(n5) - C(n0) - C(n1) - C(n2)	55.3	55.9
O(n0) - C(n0) - C(n1) - C(n2)	-178.8	-179.8
O(n0) - C(n0) - C(n5) - C(n4)	178.1	179.6
C(n6) - C(n3) - C(n2) - C(n1)	-177.0	-177.4
C(n6) - C(n3) - C(n4) - C(n5)	177.7	178.5

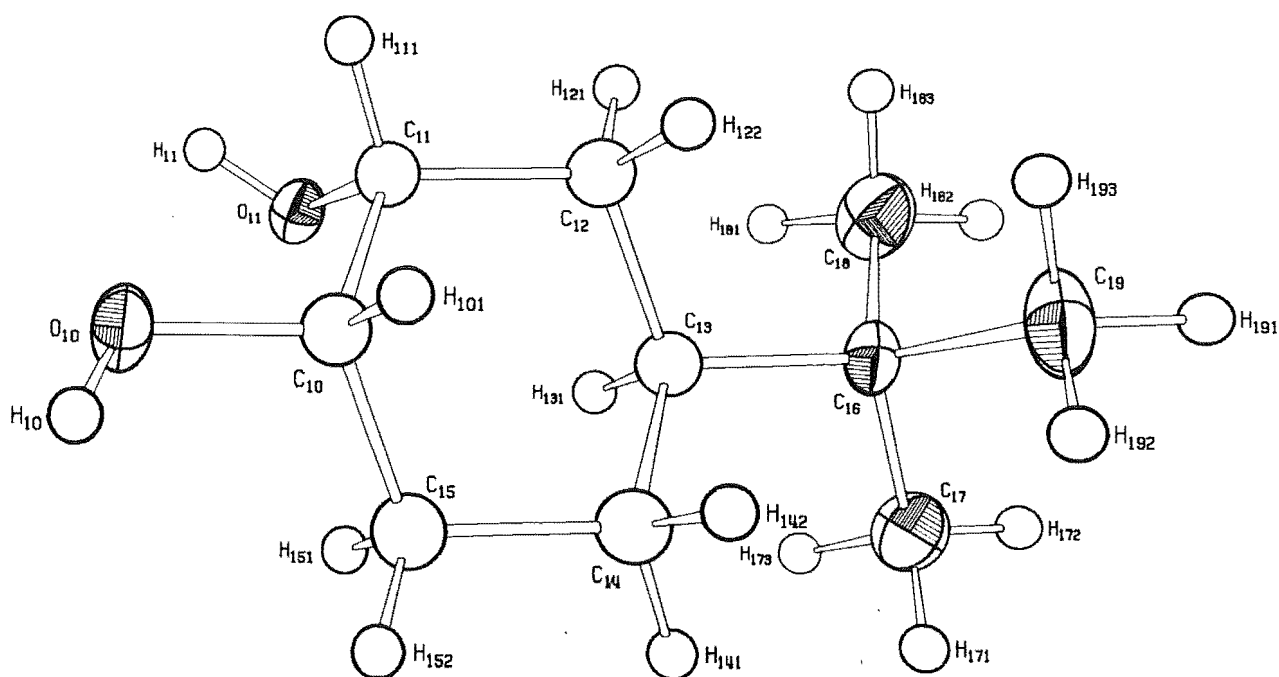


Figure 5.1 A Perspective View of the First
Independent Molecule of $C_{10}H_{20}O_2$

The C-O distances have an average value of $1.438(6)\overset{\circ}{\text{\AA}}$, which agrees well with the values found for myo-inositol⁴⁵ ($1.429\overset{\circ}{\text{\AA}}$) and epi-inositol⁴⁶ ($1.430\overset{\circ}{\text{\AA}}$). It was noted in these two compounds that the longer C-O distances are associated with oxygen atoms involved in more than two hydrogen bonds, as is the case for O (11) in this analysis. Although the difference for a particular compound is small, it must be considered to be real as it has been observed a number of times.

The average endocyclic angle is 111.0° , which is similar to the values found for myo-inositol⁴⁵ (110.7°), epi-inositol⁴⁶ (110.0°), cyclohexane-1,1-diacetic acid⁴⁷ (111.1°) and cyclo-hexylamine hydrochloride⁴⁸ (111.3°). The angles within the t-butyl group are significantly lower at 107.8° and 107.9° for the two independent molecules. This distortion, and also the long exocyclic bonds are consistent with the steric bulk of the t-butyl groups.

It can be seen from the torsion angles about the C-C bonds, as listed in Table 5.5, that there is a tendency for the cyclohexane rings to be flattened. The mean value is 55.9° which is significantly lower than the strain free value of 60° ⁴⁶. The values found for myo-inositol⁴⁵ and epi-inositol⁴⁶ are 56.8 and 56.3°

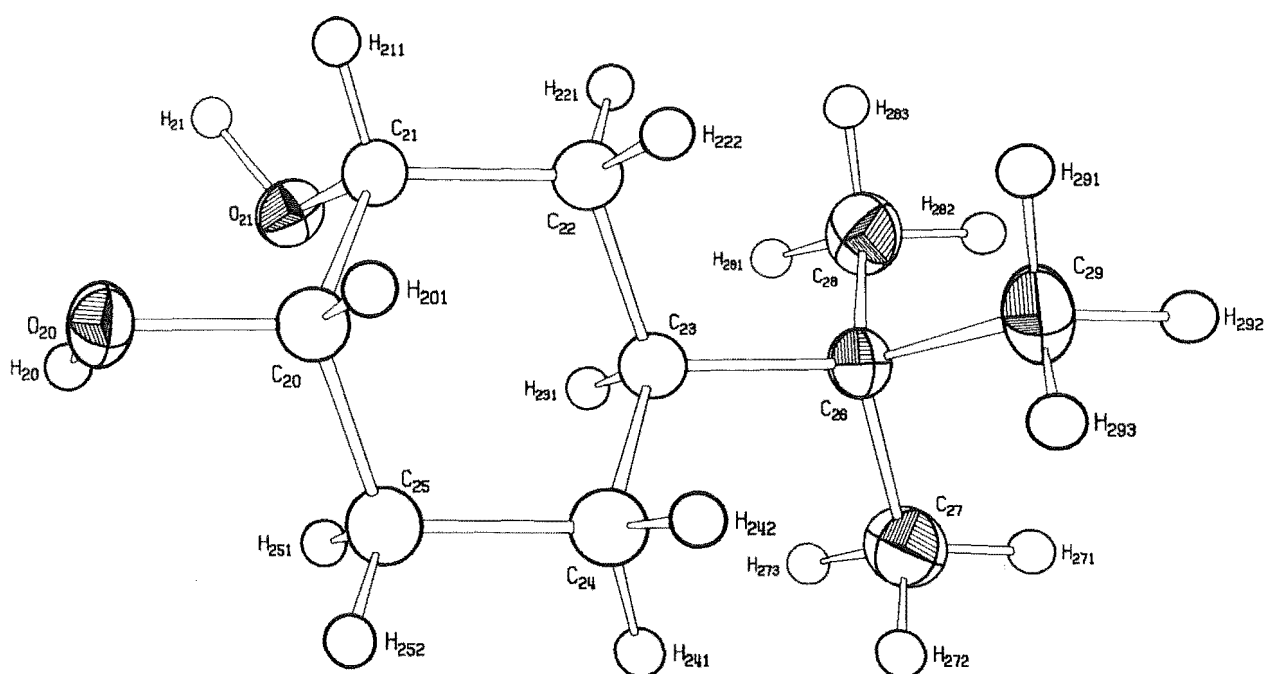


Figure 5.2 A Perspective View of the Second
Independent Molecule of $C_{10}H_{20}O_2$

respectively. Another way of measuring this effect is to examine the angles between the normals to the three planes which define chain conformation of the cyclohexane rings. The angles between the plane defined by C11, C12, C14 and C15 and the planes defined by C15, C10, C11 and C12, C13, C14 are 51.0° and 49.3° as compared to a value of 49.2° calculated for strain-free cyclohexane. The corresponding angles for the second independent molecule are 50.8° and 49.8° .

The geometry of the two independent molecules is the same within experimental error, except for the relative orientations of the atoms H(10) and H(20). This difference is readily explained in terms of the intermolecular hydrogen bonding. The crystal structure consists of groups of four molecules which are extensively hydrogen bonded together to form discrete chains parallel to the crystallographic c axis. Each group contains four molecules, with a centre of symmetry relating two sets of the two independent molecules. The hydrogen bonds linking different groups together involve H(20), whereas atom H(10) is involved in hydrogen bonding only within the groups of four molecules. There are four unique bonds in all, labelled A, B, C and D in Figure 5.3. The low

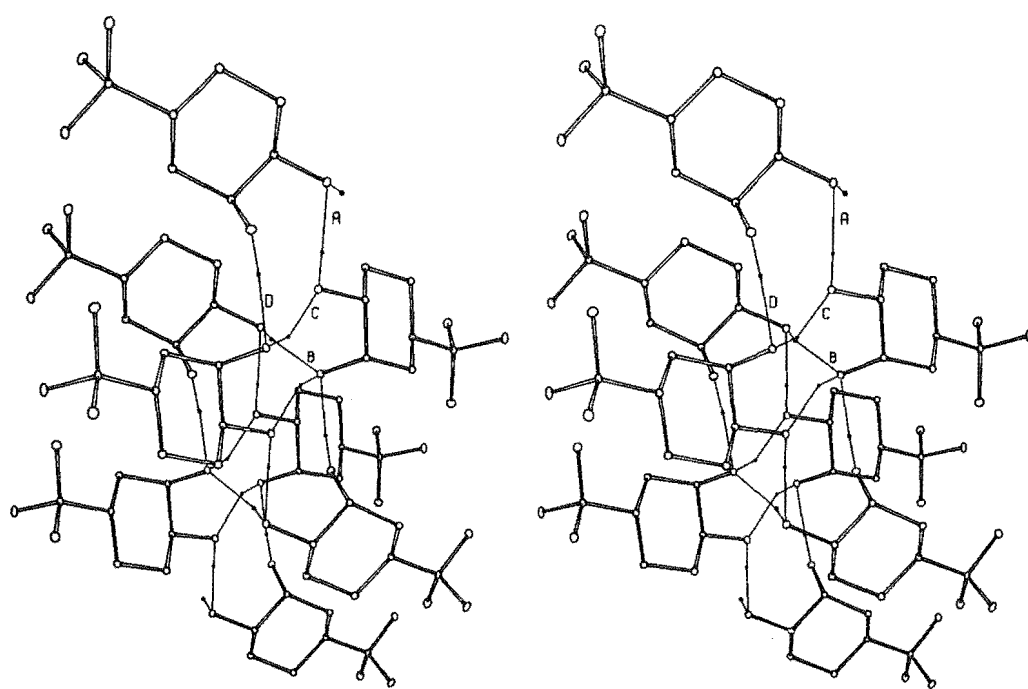


Figure 5.3 A Stereoscopic View of the Contents of
Two Unit Cells of $C_{10}H_{20}O_2$

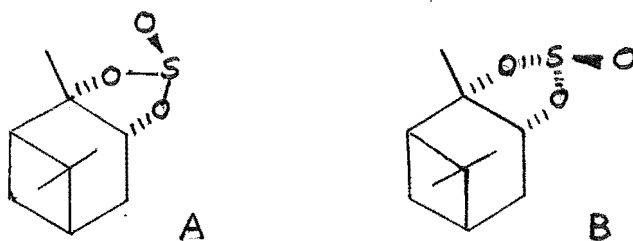
precision of the hydrogen atom positions precludes any detailed analysis of the hydrogen bonding. The O - H ... O distances are 2.77, 2.77, 2.87, 2.90 Å, all within the range found for unsymmetric hydrogen bonds⁴⁹. The chains of molecules are discrete in that there are no nonbonded contacts between nonhydrogen atoms less than 3.5 Å.

CHAPTER VI

Crystal Structures of Two Isomers of $C_{10}H_{16}SO_3$

6.1 Experimental

The samples of these two cyclic sulphites (isomers A and B) were supplied by Prof. M.P. Hartshorn.



A sample of isomer A was sublimed to give colourless well formed crystals, one of which was sealed in a capillary tube, as the compound sublimed spontaneously at room temperature over a period of a few days. An optically active sample of isomer B was obtained by re-crystallisation from pentane. This procedure was repeated until the proton magnetic resonance spectrum showed less than five per cent of isomer A present. One crystal of this sample was sealed in a capillary tube for intensity collection. Densities were not measured for either compound as the liquids used to form a density gradient column dissolved the samples before an accurate observation could be made. Unit cell

dimensions and intensity data were obtained for both compounds as described in Chapter II. The details for each compound are now outlined.

Isomer A (M.P. 50-52°C).

Crystallographic Data - $C_{10}H_{16}SO_3$, F.W. 216.3 is triclinic with $a = 7.417$ (3), $b = 10.904$ (4), $c = 7.127$ (2) Å, $\alpha = 109.01$ (2), $\beta = 95.04$ (2), $\gamma = 90.96$ (2)°; $V = 542$ Å³; $Z = 2$; $d_{calc} = 1.21$ g cm⁻³; $\mu(Mo-K\alpha) = 2.76$ cm⁻¹.

Possible space groups are $C_1^1 - P_1$ or $C_1^1 - P \bar{1}$. The centrosymmetric space group $P \bar{1}$ was confirmed by the successful structure solution and refinement. Unit cell dimensions were obtained at room temperature ($23 \pm 2^\circ C$) using Mo-K α radiation ($\lambda = 0.7107$ Å). Diffraction data were obtained from a crystal fragment whose shape approximated to that of a parallelepiped with faces defined by the forms {010}, {001}, and {100}. The perpendicular distances between these pairs of opposite faces were 0.1, 0.37 and 0.25 mm respectively. Data were collected, using Zr filtered Mo-K α radiation and a scan range of 1.6° in 2θ composed of 80 one second steps with 20 second background counts. The intensities of 2474 reflections (both hkl and $\bar{h}\bar{k}\bar{l}$) were recorded and after averaging of equivalent reflections the data set comprised 1339 independent

observations of which only 657 had $I \geq 1.5 \sigma(I)$. The factor 'p' in the expression for $\sigma(I)$ had a final value of 0.075. Absorption corrections were applied and the transmission factors ranged from 0.939 to 0.974 for the $0 \bar{1} 0$ and $\bar{2} 1 0$ reflections respectively.

Isomer B (M.P. 102°C).

Crystallographic Data - $\text{C}_{10}\text{H}_{16}\text{SO}_3$, F.W. 216.3 is orthorhombic with $a = 11.983 (1)$, $b = 12.625 (1)$, $c = 7.162 (1) \text{ \AA}$; $V = 1084 \text{ \AA}^3$; $Z = 4$; $d_{\text{calc}} = 1.32 \text{ g cm}^{-3}$; $\mu(\text{Cu-K}\alpha) = 24.28 \text{ cm}^{-1}$. The observed extinctions; $h00$, $h = 2n+1$; $0k0$, $k = 2n+1$; and $00l$, $l = 2n+1$ uniquely defined the space group as $\underline{D}_2^4 - \underline{P} 2_12_12_1$. Unit cell dimensions were obtained at room temperature ($23 \pm 2^\circ\text{C}$) using $\text{Cu-K}\alpha_1$ radiation ($\lambda = 1.5405 \text{ \AA}$).

The crystal used for collection of diffraction data was approximately a sphere of radius of 0.225 mm. Data were collected with Ni filtered $\text{Cu-K}\alpha$ radiation using two scan ranges. The first was used for data in the range $0 < 2\theta \leq 96^\circ$ and had a width of 1.6° in 2θ composed of 80 one second steps. The second was for data in the range $96 < 2\theta \leq 126^\circ$ and was of width 2.0° in 2θ with 100 steps of 0.8 seconds each. Background counts in these two ranges were of 15 seconds duration. The intensities of 5134 reflections (including all members of the form $\{hkl\}$ except $\bar{h}\bar{k}\bar{l}$ and $\bar{h}k\bar{l}$) were

recorded and after averaging of equivalent reflections the data set consisted of 1760 independent observations of which 1643 had $I \geq \sigma(I)$. The factor 'p' had a final value of 0.075. Spherical Absorption corrections were applied before the final refinements.

6.2 Solution and Refinement

Although the manner of structure solution differed for the two compounds, the refinement was similar for both, the details of which are given in Chapter III. For both compounds corrections were made for the anomalous scattering of the S atom. The course of each structure solution is now outlined.

Isomer A: The structure of this compound was first solved using a data set collected by film techniques. The SO_3 group was located from a Patterson synthesis and normal difference Fourier techniques revealed the rest of the structure. The final values for R_1 and R_2 based on a partially refined model were 0.180 and 0.222 respectively. A new data set was collected on the diffractometer and refinement continued giving values for R_1 and R_2 of 0.088 and 0.121 respectively. The positions of all hydrogen atoms were determined from a difference Fourier synthesis based on this model. The positional and thermal parameters of these atoms were

included as variables in the refinement which converged with values for R_1 and R_2 of 0.063 and 0.062 respectively. Shifts in the last cycle of refinement were all less than one tenth of their estimated standard deviations. The weighting scheme was satisfactory as average values of the minimised function showed no systematic dependence on $|F_O|$ or $\sin \theta/\lambda$. A structure factor calculation using the 652 data considered to be unobserved (those for which $I \leq 1.5 \sigma(I)$), showed no anomalies of the type $|F_c| \gg |F_O|$. The positional and thermal parameters obtained from the final cycle of least-squares refinement are listed in Table 6.1. A listing of the observed and calculated structure amplitudes for those data included in the refinement is given in Appendix B. Root-mean-square amplitudes of vibration for the anisotropic atoms are given in Table 6.2.

Isomer B: Following unsuccessful attempts to solve this problem by the Patterson methods outlined for Isomer A, the structure was determined by application of both the sum of angles formula and the tangent formula. The origin was determined by assigning phases to three reflections, 0 5 5 ($\pi/2$), 1 7 0 ($\pi/2$), and 5 0 6 (0). One of the two possible enantiomorphs was assumed by fixing the phase for the reflection 5 8 0

($\pi/2$). In addition, symbolic phases were assigned to three reflections to facilitate the manual application of the sum of angles formula. They were 2 5 6 (a), 5 9 1 (b), and 6 2 0 (c). Repeated application of the sum of angles formula to those reflection data having $|E| \geq 1.7$ resulted in symbolic phases being determined for about 40 reflections, with some indications as to the values of the symbols. The most probable values were $a = \pi/2$, $b = \pi/4$, and $c = 0$. There were contradictions in the possible value of b , both 0 and $\pi/2$ appearing possible, so a value of $\pi/4$ was used to start with. These data were input to a tangent refinement program⁵⁰ where the phases were refined, and phases were determined for an additional 200 data having $|E| \geq 1.1$. A Fourier synthesis, using as coefficients the phased $|E|$ values, revealed a partial structure of six atoms; the sulphur, three oxygens, and two carbons. Least-squares refinement of the isotropic thermal parameters of these atoms with fixed positional parameters and overall scale factor gave a value for R_1 of 0.497. Phases from this partial structure were accepted as starting phases for a second tangent refinement if they satisfied two criteria:

- 1) they were associated with reflections which had $|E| \geq 1.5$

2) that $|F_c| \geq 0.3|F_0|$ as obtained from the refined partial model.

The phases for 36 reflections were obtained in this way and the tangent refinement resulting from these starting values gave a final R-Karle value of 0.277. This recycling procedure using the tangent formula has been described elsewhere²⁷.

The E-map resulting from this last tangent refinement revealed 13 of the 14 non-hydrogen atoms in the asymmetric unit. (It was subsequently found that 3 of the atoms of the earlier partial structure were in fact spurious peaks.) A difference Fourier synthesis revealed the last atom. Least-squares refinement of the 'heavy atom' model converged with values for R_1 and R_2 of 0.080 and 0.120 respectively. All of the hydrogen atoms were located from a difference Fourier synthesis and their positional and isotropic thermal parameters were included as variables in further refinement, which converged with values for R_1 and R_2 of 0.063 and 0.089 respectively. The thermal motion of the SO_3 group was converted to an anisotropic model for these calculations.

To determine the absolute configuration of the molecule the inverse model was refined for one further cycle. This produced values for R_1 and R_2 of 0.051 and

0.071, a significant difference. The coordinates of this inverse model were subsequently used in all further calculations. In the final refinement, which converged with values of 0.049 and 0.063 for R_1 and R_2 respectively, the methyl carbon atoms were also assigned anisotropic thermal parameters.

Shifts in the final cycle of least-squares refinement were all less than one tenth of their estimated standard deviations. The weighting scheme was satisfactory as average values of the minimised function showed no systematic dependence on $|F_O|$ or $\sin \theta/\lambda$. A structure factor calculation, using the 117 data considered to be unobserved, i.e. those for which $I \leq \sigma(I)$, showed no anomalies of the type $|F_c| \gg |F_O|$.

The positional and thermal parameters obtained from the final cycle of least-squares refinement are listed in Table 6.3. A listing of the observed and calculated structure amplitudes for those data included in the refinement is given in Appendix B. Root-mean-square amplitudes of vibration for the anisotropic atoms are given in Table 6.4. For both structures information concerning the mean planes through selected groups of atoms, is summarised in Table 6.9.

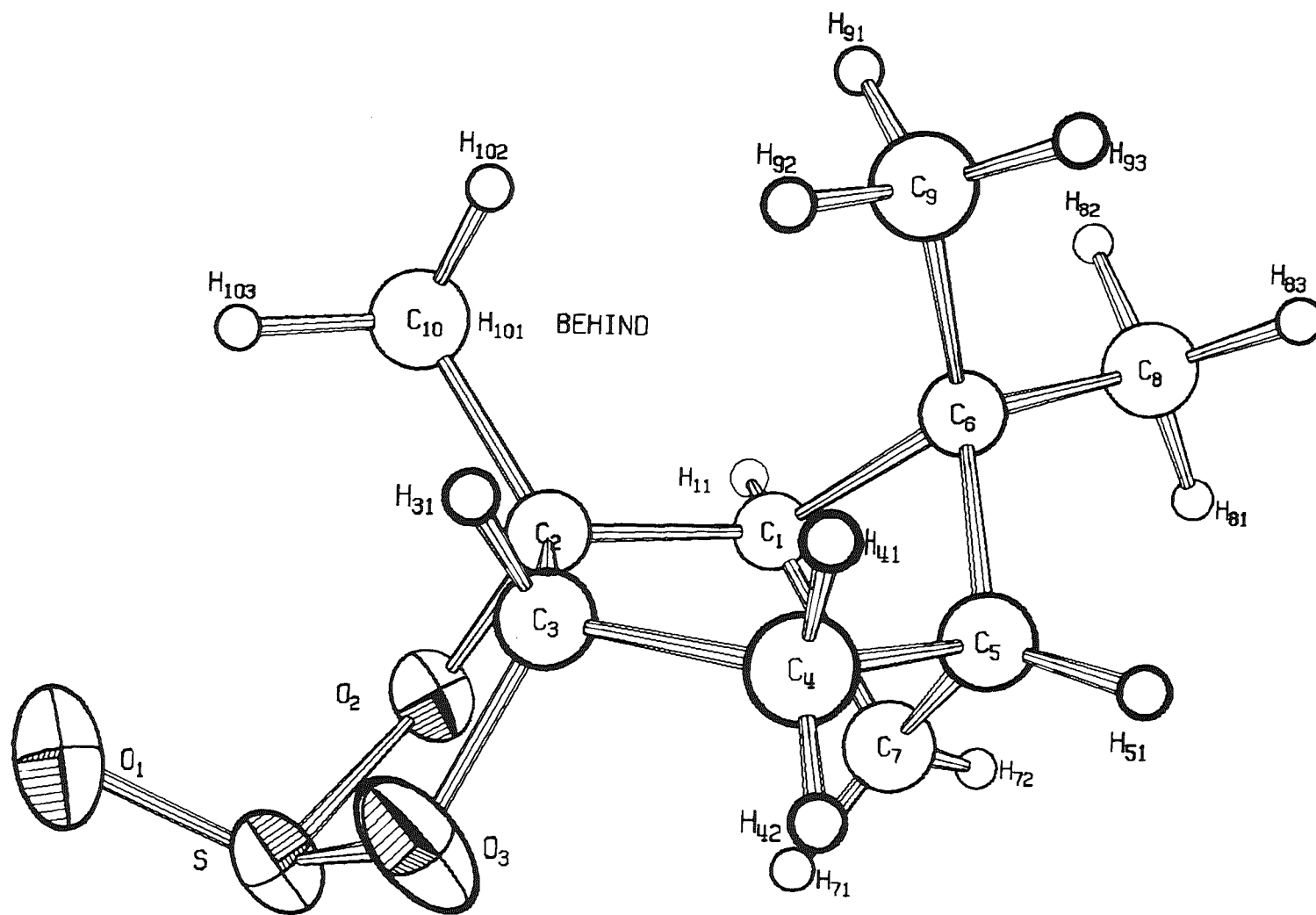
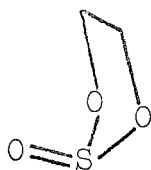


Figure 6.1 A Perspective View of $C_{10}H_{16}SO_3(A)$

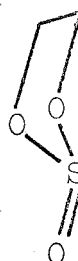
6.3 Description of Structures and Discussion

The crystal structures of these two isomers consist of well separated monomeric units. The minimum non-bonded inter-molecular contacts are 3.43 and 3.37 Å for isomers A and B respectively. A summary of intra-molecular bonding distances and angles for both isomers is given in Tables 6.5 to 6.8. Figures 6.1 and 6.3 define the atom numbering system. Figures 6.2 and 6.4 are stereoscopic views of each molecule.

The molecular structures of these two compounds are normal in that there are no unusual bonding distances or angles. The geometrical isomerism arises from the different conformations of the five membered sulphite rings. The sulphur atom can be positioned in one of two ways with respect to this ring; α (below) or β (above). The exocyclic oxygen atom can adopt two conformations; quasi-axial (I) or quasi-equatorial (II), as described in Dansted's thesis.⁵¹



I



II

TABLE 6.1

POSITIONAL AND THERMAL PARAMETERS^a FOR C₁₀H₁₆SO₃ (A)

Atom	x	y	z	U ₁₁	U ₂₂	U ₃₃	U ₁₂	U ₁₃	U ₂₃
S	0.6299(4)	0.7626(3)	0.7754(4)	0.06858	0.08445	0.06342	0.00429	-0.00977	0.03384
O(1)	0.754(1)	0.6589(7)	0.731(1)	0.09526	0.10771	0.12961	0.02858	-0.00974	0.06270
O(2)	0.6070(7)	0.8165(5)	0.5915(8)	0.05888	0.06220	0.06270	-0.00017	-0.00227	0.02771
O(3)	0.4331(9)	0.6979(7)	0.7310(9)	0.07030	0.14793	0.07878	-0.01744	-0.01547	0.07472

Table 6.1 (contd.)

Atom	x	y	z	B(\AA^2)
C(1)	0.363(1)	0.8400(7)	0.369(1)	3.6(2)
C(2)	0.473(1)	0.7410(7)	0.430(1)	4.0(2)
C(3)	0.359(1)	0.6623(9)	0.524(1)	4.4(2)
C(4)	0.156(1)	0.6868(9)	0.522(2)	5.1(2)
C(5)	0.109(1)	0.8005(8)	0.449(1)	4.4(2)
C(6)	0.178(1)	0.7831(7)	0.247(1)	3.8(2)
C(7)	0.250(1)	0.9096(9)	0.541(1)	4.8(2)
C(8)	0.100(2)	0.876(1)	0.145(2)	5.3(2)
C(9)	0.159(2)	0.6472(9)	0.092(2)	5.3(2)
C(10)	0.583(2)	0.657(1)	0.267(2)	5.6(2)
H(11)	0.449(9)	0.888(6)	0.306(9)	4(2)
H(31)	0.368(9)	0.576(7)	0.45(1)	5(2)
H(41)	0.091(9)	0.601(6)	0.433(9)	3(1)
H(42)	0.88(1)	0.293(7)	0.36(1)	6(2)
H(51)	0.98(1)	0.807(6)	0.468(9)	4(2)

Table 6.1 (contd.)

Atom	x	y	z	B(\AA^2)
H(71)	0.694(8)	0.083(5)	0.328(9)	3(2)
H(72)	0.77(1)	0.010(9)	0.47(1)	7(2)
H(81)	0.090(9)	0.965(7)	0.24(1)	5(2)
H(82)	0.182(9)	0.870(6)	0.02(1)	4(2)
H(83)	0.965(9)	0.848(6)	0.092(9)	4(2)
H(91)	0.24(1)	0.634(6)	-0.01(1)	4(2)
H(92)	0.201(9)	0.580(7)	0.16(1)	5(2)
H(93)	0.03(1)	0.629(6)	0.047(9)	3(2)
H(101)	0.639(8)	0.713(6)	0.231(9)	3(2)
H(102)	0.502(8)	0.604(6)	0.151(9)	3(1)
H(103)	0.68(1)	0.594(8)	0.32(1)	7(2)

^aThe temperature factor expression for the anisotropic atoms is

$$\exp[-2\pi^2(U_{11}h^2a^{*2} + U_{22}k^2b^{*2} + U_{33}l^2c^{*2} + 2U_{12}hka^*b^* + 2U_{13}hla^*c^* + 2U_{23}klb^*c^*)]$$

TABLE 6.2
ROOT MEAN SQUARE AMPLITUDES OF VIBRATION (\AA)
FOR $\text{C}_{10}\text{H}_{16}\text{SO}_3$ (A)

Atom	Min.	Int.	Max.
S	0.211(4)	0.283(4)	0.297(4)
O(1)	0.227(9)	0.353(9)	0.378(9)
O(2)	0.223(8)	0.240(8)	0.270(8)
O(3)	0.202(9)	0.261(9)	0.407(9)

TABLE 6.3

POSITIONAL AND THERMAL PARAMETERS^a FOR C₁₀H₁₆SO₃ (B)

Atom	x	y	z	U ₁₁	U ₂₂	U ₃₃	U ₁₂	U ₁₃	U ₂₃
S	0.9674(1)	0.9852(1)	0.0211(1)	0.07473	0.06144	0.06442	0.01382	0.00091	0.00597
O(1)	0.9639(2)	0.0028(2)	0.2184(3)	0.10675	0.09221	0.06170	0.00683	-0.00972	0.01293
O(2)	0.0020(2)	0.0946(2)	0.9223(3)	0.05989	0.06918	0.06671	0.00731	0.00356	0.01264
O(3)	0.8421(2)	0.9871(2)	0.9416(4)	0.07942	0.04865	0.07937	-0.00063	-0.01073	0.00476
C(8)	0.7201(4)	0.3004(3)	0.7022(6)	0.08020	0.06561	0.07221	0.00989	-0.01290	0.00132
C(9)	0.1981(5)	0.9391(3)	0.6006(8)	0.10357	0.04983	0.08082	0.00697	0.00602	-0.00066
C(10)	0.9352(6)	0.1417(5)	0.6179(6)	0.11634	0.08334	0.05021	0.01866	0.02081	0.00441

Table 6.3 (contd.)

Atom	x	y	z	B(\AA^2)
C(1)	0.0881(3)	0.7645(3)	0.6049(5)	4.27(6)
C(2)	0.9114(3)	0.1513(2)	0.8254(5)	4.14(6)
C(3)	0.8043(3)	0.0926(2)	0.8797(5)	4.29(6)
C(4)	0.7693(4)	0.8527(3)	0.5258(6)	5.27(7)
C(5)	0.7362(3)	0.7380(3)	0.5593(5)	4.66(7)
C(6)	0.2061(3)	0.8188(2)	0.6273(4)	4.28(6)
C(7)	0.1128(3)	0.7659(3)	0.3931(5)	4.99(7)
H(11)	0.968(3)	0.313(3)	0.829(6)	6.1(9)
H(31)	0.759(3)	0.086(3)	0.756(6)	6.7(9)
H(41)	0.759(3)	0.888(3)	0.645(5)	5.3(8)
H(42)	0.836(4)	0.859(3)	0.473(6)	7(1)
H(51)	0.792(5)	0.712(4)	0.644(8)	10(1)
H(71)	0.589(3)	0.658(3)	0.674(6)	5.6(8)
H(72)	0.574(2)	0.792(2)	0.650(4)	3.3(6)
H(81)	0.703(3)	0.230(3)	0.656(5)	5.1(8)
H(82)	0.760(3)	0.335(3)	0.577(6)	5.4(8)
H(83)	0.651(4)	0.332(4)	0.718(6)	7(1)
H(91)	0.667(4)	0.550(4)	0.519(7)	8(1)
H(92)	0.694(5)	0.465(5)	0.891(9)	12(2)
H(93)	0.838(3)	0.475(4)	0.800(7)	7(1)
H(101)	0.001(4)	0.170(3)	0.595(6)	5(1)
H(102)	0.887(3)	0.183(3)	0.535(5)	4.5(8)
H(103)	0.949(4)	0.087(4)	0.593(6)	6(1)

^aAs for Table 6.1

TABLE 6.4
ROOT MEAN SQUARE AMPLITUDES OF VIBRATION (\AA)
FOR $\text{C}_{10}\text{H}_{16}\text{SO}_3$ (B)

Atom	Min.	Int.	Max.
S	0.226(1)	0.255(1)	0.290(1)
O(1)	0.233(3)	0.310(3)	0.332(4)
O(2)	0.232(3)	0.242(3)	0.289(3)
O(3)	0.219(2)	0.263(3)	0.301(3)
C(8)	0.238(5)	0.264(5)	0.303(5)
C(9)	0.221(4)	0.282(5)	0.325(5)
C(10)	0.210(5)	0.275(6)	0.361(7)

TABLE 6.5
BOND DISTANCES (\AA) FOR $\text{C}_{10}\text{H}_{16}\text{SO}_3$ (\AA)^a

S-O(1)	1.44(1)	C(1)-C(2)	1.51(1)
		C(2)-C(3)	1.53(1)
S-O(2)	1.57(1)	C(2)-C(10)	1.53(1)
S-O(3)	<u>1.60(1)</u>	C(3)-C(4)	1.53(1)
	1.59(1)	C(4)-C(5)	1.53(1)
		C(5)-C(6)	1.53(1)
O(2)-C(2)	1.47(1)	C(5)-C(7)	1.51(1)
O(3)-C(3)	<u>1.45(1)</u>	C(6)-C(1)	1.56(1)
	1.46(1)	C(6)-C(8)	1.52(1)
		C(6)-C(9)	1.53(1)
		C(7)-C(1)	<u>1.54(1)</u>
			1.53(2)

^aThe figures in parentheses are e.s.d.'s in the last significant figure. Mean values are calculated using the expression

$$\bar{l} = \Sigma(l_i/\sigma_i^2)/\Sigma(1/\sigma_i^2)$$

The e.s.d. of the mean value is calculated as a root mean square deviation using the expression

$$\sigma(\bar{l}) = [\Sigma(\bar{l}-l_i)^2/(N-1)]^{1/2}$$

TABLE 6.6

BOND ANGLES (DEGREES) FOR $C_{10}H_{16}SO_3$ (A)^a

O(1)-S-O(2)	108.8(4)	C(6)-C(1)-C(7)	86.0(6)
O(1)-S-O(3)	107.2(4)	C(6)-C(5)-C(7)	88.4(7)
O(2)-S-O(3)	93.5(3)	C(8)-C(6)-C(9)	107.0(7)
C(2)-O(2)-S	113.7(4)	C(8)-C(6)-C(5)	113.8(7)
C(3)-O(3)-S	114.4(5)	C(8)-C(6)-C(1)	110.4(7)
		C(9)-C(6)-C(5)	117.5(7)
C(1)-C(2)-C(3)	111.9(7)	C(9)-C(6)-C(1)	121.7(7)
C(2)-C(3)-C(4)	116.3(7)		
C(3)-C(4)-C(5)	112.1(8)	C(10)-C(2)-C(1)	114.4(7)
		C(10)-C(2)-C(3)	113.3(8)
C(6)-C(1)-C(2)	113.6(6)	C(10)-C(2)-O(2)	105.6(7)
C(7)-C(1)-C(2)	108.3(7)		
C(6)-C(5)-C(4)	111.3(7)	C(1)-C(6)-C(5)	85.5(6)
C(7)-C(5)-C(4)	109.0(8)	C(1)-C(7)-C(5)	86.9(7)

^aAs for Table 6.5, but e.s.d.'s for the mean values were not calculated as they are much larger than an e.s.d. for an individual value.

TABLE 6.7

BOND DISTANCES (Å) FOR C₁₀H₁₆SO₃ (B)^a

S-O(1)	1.432(3)
S-O(2)	1.606(2)
S-O(3)	<u>1.604(3)</u>
	1.605(1)
C(2)-O(2)	1.473(4)
C(3)-O(3)	<u>1.474(3)</u>
	1.474(1)
C(1)-C(2)	1.514(5)
C(2)-C(3)	1.531(5)
C(2)-C(10)	1.517(5)
C(3)-C(4)	1.532(5)
C(4)-C(5)	1.520(5)
C(5)-C(6)	1.559(5)
C(5)-C(7)	1.516(5)
C(6)-C(1)	1.578(5)
C(6)-C(8)	1.525(5)
C(6)-C(9)	1.533(5)
C(7)-C(1)	<u>1.545(5)</u>
	1.53(2)

^aAs for Table 6.5

TABLE 6.8

BOND ANGLES (DEGREES) FOR $C_{10}H_{16}SO_3$ (B)^a

O(2)-S-O(3)	94.2(2)	C(6)-C(1)-C(7)	85.6(3)
		C(6)-C(5)-C(7)	87.3(3)
O(1)-S-O(2)	108.0(2)	C(1)-C(6)-C(5)	85.4(2)
O(1)-S-O(3)	<u>108.7(2)</u>	C(1)-C(7)-C(5)	88.0(3)
	108.4		
		C(1)-C(6)-C(8)	122.3(3)
C(1)-C(2)-C(3)	112.1(3)	C(1)-C(6)-C(9)	111.2(3)
C(2)-C(3)-C(4)	115.9(3)	C(5)-C(6)-C(8)	118.8(3)
C(3)-C(4)-C(5)	112.1(3)	C(5)-C(6)-C(9)	111.3(3)
C(6)-C(1)-C(2)	111.9(3)	C(8)-C(6)-C(9)	106.7(3)
C(6)-C(5)-C(4)	111.3(3)		
C(7)-C(1)-C(2)	109.5(3)	C(10)-C(2)-O(2)	106.5(3)
C(7)-C(5)-C(4)	108.7(3)	C(10)-C(2)-C(3)	111.6(4)
		C(10)-C(2)-C(1)	113.4(3)
C(2)-O(2)-S	115.8(2)		
C(3)-O(3)-S	<u>114.0(2)</u>		
	114.9		

^a As for Table 6.6

TABLE 6.9
MEAN PLANES

Plane	Atoms through which mean plane is calculated
I	O(2), O(3), C(2), C(3) of isomer A
II	C(1), C(2), C(4), C(5) of isomer A
III	O(2), O(3), C(2), C(3) of isomer B
IV	C(1), C(2), C(4), C(5) of isomer B

Deviations (Å)

Atom	Plane I	Plane II	Plane III	Plane IV
S	0.451		-0.223	
O(1)	1.892		-1.598	
O(2)	0.002		-0.076	
O(3)	-0.002		0.076	
C(1)		0.014		-0.001
C(2)	-0.003	-0.011	0.117	0.001
C(3)	0.003	-0.087	-0.117	0.169
C(4)		0.011		-0.001
C(5)		-0.014		0.001

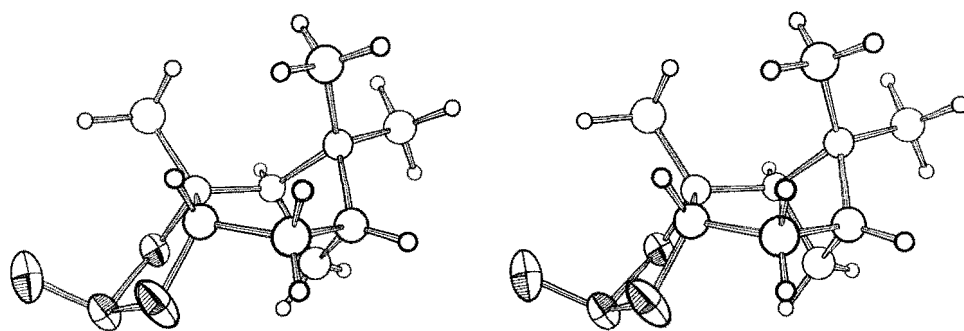
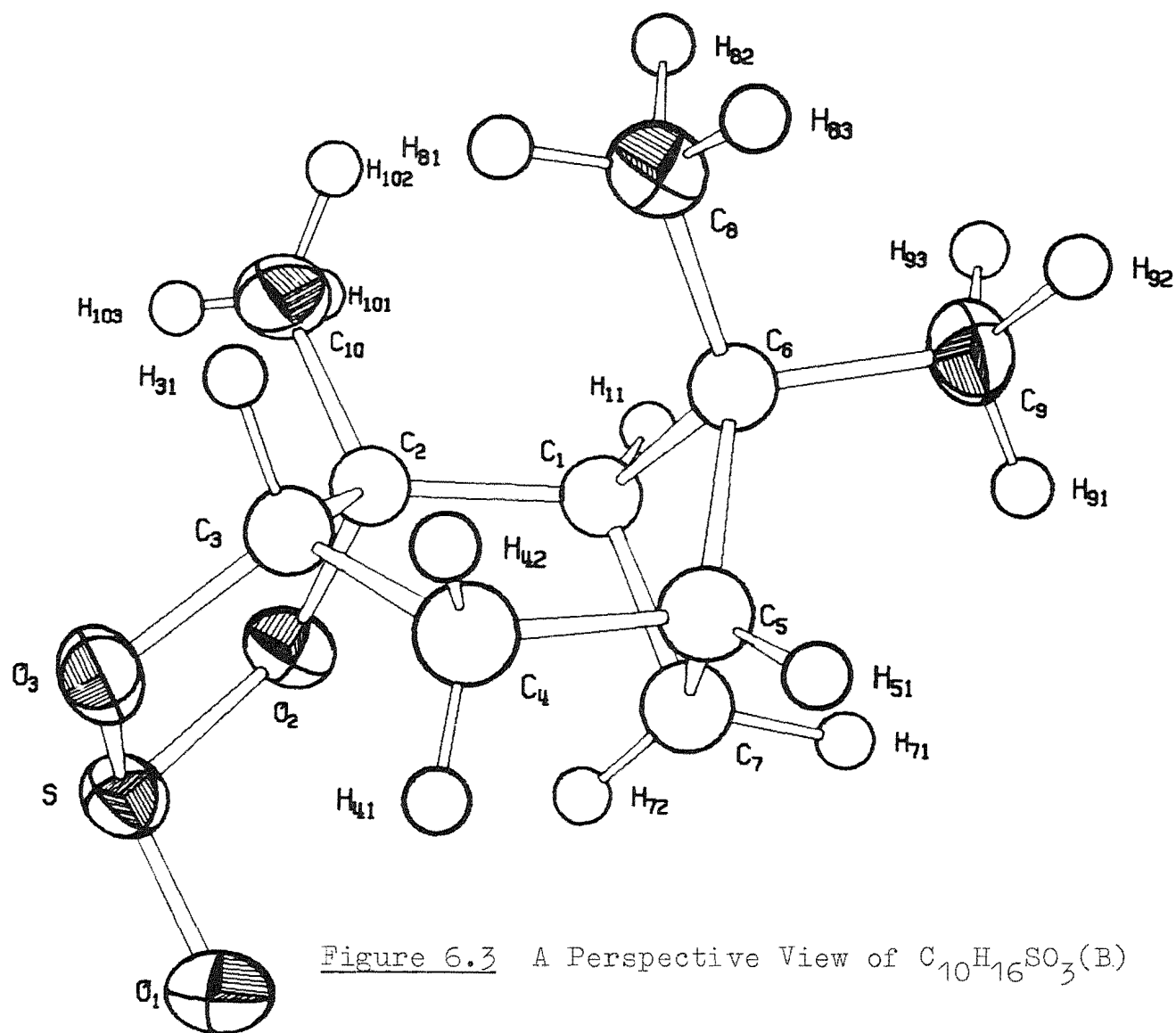


Figure 6.2 A Stereoscopic View of
 $C_{10}H_{16}SO_3(A)$

Dansted⁵¹ had attempted to predict the stereochemistry of the sulphite rings by interpretation of the proton magnetic resonance spectra of these two compounds. As the C(10) methyl group was shielded in isomer B with respect to isomer A (assumed due to the magnetic anisotropy of the S = O bond), it was argued that the terminal oxygen atom of the B isomer was quasi-equatorial (II). The buckling of the ring system at C(3) was also predicted from the relationship between the coupling constants and dihedral angles for the 3 β hydrogen atom.

The results of these structure analyses only partially confirm the predictions made by Dansted. It has been found that in the A isomer the sulphur atom is β (above) with respect to the sulphite ring and the terminal oxygen atom is quasi-axial (I). In isomer B the terminal oxygen atom is again quasi-axial (I), with the sulphur atom α (below) to the sulphite ring, although not as far below as it was above in isomer A (0.22 Å versus 0.451 Å). The buckling at atom C(3) can be described in terms of the deviation of this atom from the mean plane through atoms C(1), C(2), C(4) and C(5).

This group of atoms is not planar in isomer A (Plane II) with atom C(3) 0.087 Å below the mean plane.



This has resulted in the bonds C(2)-O(2) and C(3)-O(3) being twisted with respect to one another as shown by the deviations of the atoms from the mean plane through O(2), O(3), C(2) and C(3) (Plane I), which has a χ^2 value of 0.41. In isomer B the buckling is greater as the deviation of C(3) from the mean plane (Plane IV) is 0.169 Å. This is also reflected by the mean plane through the atoms C(2), O(2), C(3) and O(3) (Plane III) which has a χ^2 value of 4224 (i.e. those atoms are not planar).

It may also be noted that a movement of C(3) to a position above or below the mean plane results in a movement of the C(10) methyl group away from or towards the nearer of the two gem-methyl groups bonded to atom C(6). This is confirmed by the closer approach of C(10) in isomer A at 3.27 Å compared to a distance of 3.82 Å for isomer B. Further evidence for this steric interaction can be obtained from a comparison of bonding angles of the type C(9) - C(6) - C(1) for isomer A and C(8) - C(6) - C(1) for isomer B with the angles C(9) - C(6) - C(5) and C(8) - C(6) - C(5) for isomers A and B respectively. The greater angle with the C(6) - C(1) bond indicates that the steric interaction between the C(10) methyl and C(9) methyl (isomer A) or C(8) methyl (isomer B) is relieved by this angle deformation.

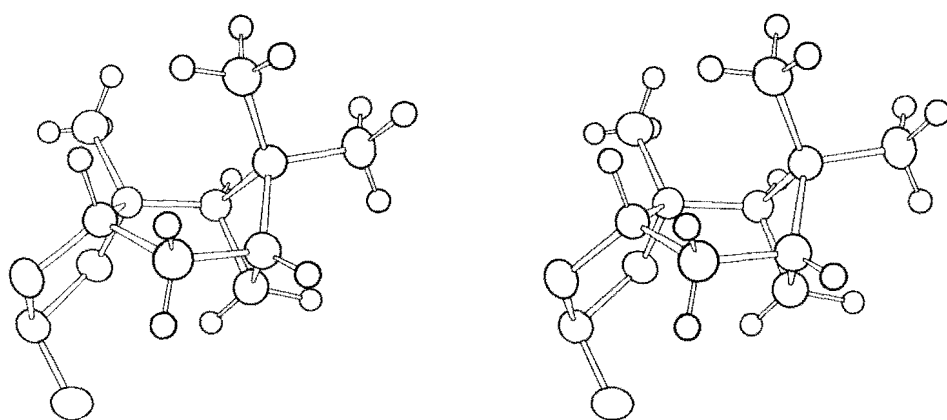


Figure 6.4 A Stereoscopic View of $C_{10}H_{16}SO_3(B)$

A comparison of the bonding distances of the two isomers reveals no differences which cannot be explained in terms of experimental error. (It is worth noting here that a comparison of the estimated standard deviations in the bond lengths and angles of the two compounds shows the increased accuracy obtainable for these type of compounds when the diffraction data is measured using Cu-K α radiation as opposed to Mo-K α radiation. The geometries of the sulphite rings are similar to that found for 2,2'-dichlorotrimethylene sulphite⁵². A comparison of the relevant bonding lengths and angles is given in Table 6.10. The only dimensions which differ are the distances of the type S-O(2) and S-O(3), and the angle O(2)-S-O(3). These differences are small but seem to be related to the different constraints of a five and six membered cyclic sulphite.

CHAPTER VII

Crystal Structure of Dibenzyl Dimedone, $C_{22}H_{24}O_2$

7.1 Experimental

Colourless well formed crystals of dibenzyl dimedone, 5,5-dimethyl-2,2-dibenzylcyclohexane-1,3-dione, were supplied by Dr M.H.G. Munro and were used without further recrystallisation. The compound was prepared by benzylation of dimedone under basic conditions.

Crystallographic Data - $C_{22}H_{24}O_2$, F.W. 320.4 is monoclinic with $a = 10.845(1)$, $b = 9.371(1)$, $c = 19.163(2)$ Å, $\beta = 109.08(1)^\circ$; $V = 1840.5$ Å³; $Z = 4$; $d_{calc} = 1.16$ g cm⁻³; $\mu(Cu-K\alpha) = 5.75$ cm⁻¹. The observed extinctions $h0l$, $l = 2n + 1$; $0k0$, $k = 2n + 1$ uniquely indicate the centrosymmetric space group $C_{2h}^5 - P2_1/c$. Unit cell dimensions and their estimated standard deviations were obtained at room temperature ($23 \pm 2^\circ C$) with Cu-K α radiation ($\lambda = 1.5418$ Å) using the least-squares procedure described in Chapter II. Diffraction data were obtained from a crystal with boundary faces defined by the forms $\{001\}$, $\{100\}$, $\{0\bar{1}2\}$, and $\{0\bar{1}\bar{2}\}$. Crystal dimensions normal to these faces were 0.125, 0.2125, 0.3375 and 0.3125 mm respectively. A

check of the crystal mosaicity showed the peak width for typical reflections to be acceptably low at 0.1° .

Data were collected using a scan range of 1.2° in 2θ composed of 60 steps of 1 second each with 15 second background counts. The intensities of 5473 reflections (including both hkl and $\bar{h}\bar{k}\bar{l}$) having $0 \leq 2\theta \leq 114^\circ$ were recorded in this way. After averaging of equivalent reflections, the data set consisted of 2477 independent observations, of which 1879 had intensities greater than their standard errors $\sigma(I)$. The value for the factor p was finally set at 0.075. Absorption corrections were applied using Gaussian integration and transmission factors ranged from 0.857 to 0.944 for the $0\bar{1}0$ and $0\bar{2}0$ reflections respectively.

7.2 Structure Solution and Refinement

The structure was solved using a combination of the symbolic addition procedure and the tangent refinement procedure. The origin was specified by assigning positive signs (a phase angle of 0.0 radians) to the three reflections $1\bar{1}\bar{1}5$, $0\bar{1}\bar{1}4$, and $1\bar{2}14$. Symbolic signs were assigned to the phases of another three reflections, the $2\bar{2}0$, $2\bar{2}14$, and $6\bar{5}\bar{1}2$, and the Σ_2 relationship was used to determine symbolic signs for the 138 data having $|E| \geq 2.0$. The tangent

formula was used to both refine and extend the phase set to include these data with $|E| \geq 1.6$. An E-map was calculated using the 284 reflections whose phases had been determined assuming values for the symbols as indicated from the symbolic addition procedure, and this revealed all of the non-hydrogen atoms in the asymmetric unit. The R-Karle value for this phase set was 0.155. Preliminary least-squares refinement gave values for R_1 and R_2 of 0.13 and 0.186 respectively. In these, and some following structure factor calculations the phenyl rings were treated as rigid groups^{53,54} and constrained to their known geometry (D_{6h} symmetry, $d(C-C) = 1.390\text{\AA}$); variable parameters for the rings included an overall isotropic thermal parameter, three orientation angles and the coordinates of the ring centre. Further refinement was carried out with an anisotropic model for the thermal motion of all but the phenyl carbon atoms. This produced values for R_1 and R_2 of 0.115 and 0.166 respectively. All of the hydrogen atoms were located from a difference Fourier synthesis calculated from this model. The methyl hydrogen atoms were included in those idealized tetrahedral positions which gave the best fit, in a least-squares sense, to appropriate Fourier peaks. With all the hydrogen atoms included in fixed positions, and isotropic temperature

factors of 8.0\AA^2 for the phenyl hydrogens and 9.0\AA^2 for the others, further refinement converged with values for R_1 and R_2 of 0.079 and 0.107 respectively. Several attempts were made to improve the model but it was not until the phenyl groups were removed from the rigid group restraint and their individual atoms assigned anisotropic temperature factors that any improvement was obtained. This refinement converged with values for R_1 and R_2 of 0.056 and 0.061 respectively. Shifts in the last cycle of refinement were all less than their estimated standard deviations. A final difference synthesis revealed peaks approximately one half the height of the last hydrogen atom taken from a similar earlier calculation. A structure factor calculation using those data considered to be unobserved ($I > \sigma(I)$) showed no anomalies of the type $|F_c| \gg |F_o|$. There was no evidence for secondary extinction and no correction was applied. The positional and thermal parameters obtained from the last cycle of least-squares refinement are given in Table 7.1. A listing of the observed and calculated structure amplitudes for those data included in the refinement is given in Appendix B. Root-mean square amplitudes of vibration are listed in Table 7.2. Information concerning the mean-planes through selected groups of atoms is summarized in Table 7.5.

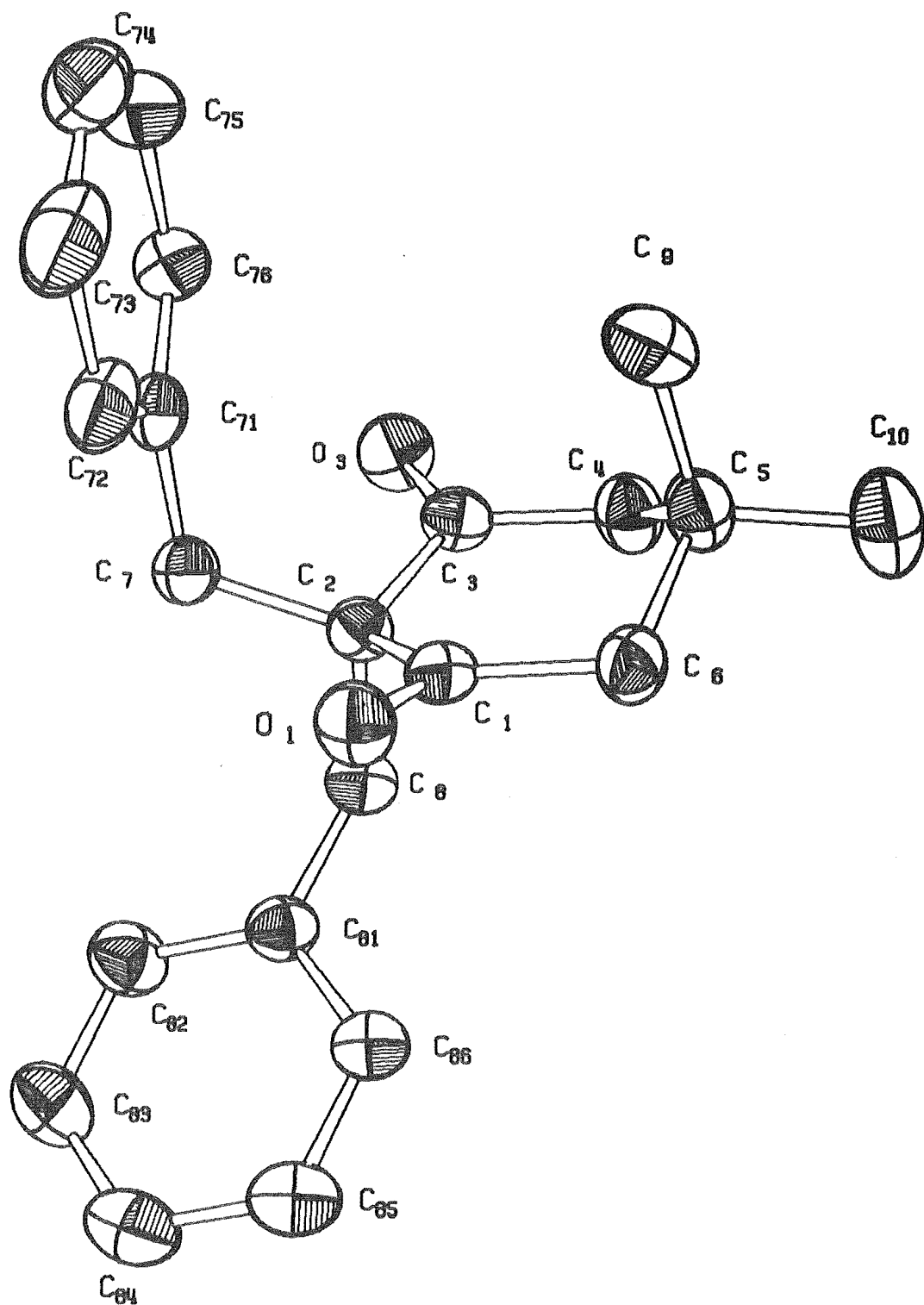


Figure 7.1 A Perspective View of $C_{22}H_{24}O_2$

7.3 Structure Description and Discussion

The crystal structure consists of well separated monomeric molecules, the shortest intermolecular non-bonded contact being 3.44°\AA . A general view of the molecule is given in Figure 7.1 showing the labelling used and Figure 7.2 is a stereoscopic representation of the structure. A summary of bond distances and angles is given in Tables 7.3 and 7.4 respectively.

The cyclohexane ring is in a chair conformation with one end considerably flattened, due to the bonding requirements of the carbonyl oxygen atoms which can be described in terms of sp^2 hybridisation of atoms C(1) and C(3). This is illustrated by examining the angles between the normals to mean-planes I, II and III. ^(Table 7.5) The angle between mean-planes I and II is 23.4° which, when compared to the value of 49.2° calculated for strain free cyclohexane⁵⁶, shows the considerable flattening induced by the 1,3 dione system. The angle between mean-planes II and III is 49.6° indicating no significant distortions of this part of the molecule.

The phenyl groups are very nearly perpendicular to each other, with a dihedral angle of 86.1° . The groups are essentially planar (Planes IV and V); no atom deviates from the best mean-plane by more than 0.005°\AA . The internal angles of both groups are all very close

TABLE 7.1
POSITIONAL AND THERMAL PARAMETERS^a FOR C₂₂O₂H₂₄

Atom	x	y	z	U ₁₁	U ₂₂	U ₃₃	U ₁₂	U ₁₃	U ₂₃
O(1)	0.5122(2)	0.3111(2)	0.2918(1)	0.06259	0.05963	0.05800	-0.01237	0.02334	0.00340
O(3)	0.3148(2)	0.0078(2)	0.4151(1)	0.07884	0.09361	0.06183	-0.01473	0.03568	0.01308
C(1)	0.4474(2)	0.2059(3)	0.2915(1)	0.04326	0.05048	0.04917	0.00212	0.02071	0.00067
C(2)	0.4577(2)	0.1293(3)	0.3634(1)	0.04614	0.05224	0.04470	-0.00141	0.01704	0.00429
C(3)	0.3363(2)	0.0419(3)	0.3589(1)	0.05366	0.05576	0.05791	0.00008	0.02379	0.00801
C(4)	0.2520(3)	-0.0141(3)	0.2854(1)	0.06316	0.06723	0.06287	-0.01782	0.01712	-0.00239
C(5)	0.2278(3)	0.0937(3)	0.2224(1)	0.05627	0.06796	0.05506	-0.01064	0.01257	-0.00258
C(6)	0.3606(2)	0.1427(3)	0.2200(1)	0.05776	0.07032	0.04426	-0.00691	0.01722	-0.00246
C(7)	0.4962(2)	0.2327(3)	0.4299(1)	0.05135	0.06209	0.04411	0.00341	0.01301	-0.00128
C(8)	0.5666(3)	0.0104(3)	0.3753(1)	0.05493	0.05511	0.06009	0.00520	0.02141	0.00862
C(9)	0.1493(3)	0.2210(4)	0.2350(2)	0.05591	0.09366	0.08820	0.00415	0.02185	0.00804
C(10)	0.1539(3)	0.0202(4)	0.1496(2)	0.08990	0.10620	0.06820	-0.02424	0.00402	-0.01130

Table 7.1 (contd.)

Atom	x	y	z	U_{11}	U_{22}	U_{33}	U_{12}	U_{13}	U_{23}
C(71)	0.4022(2)	0.3525(3)	0.4271(1)	0.05445	0.06854	0.03576	-0.00023	0.00748	-0.01034
C(72)	0.4209(3)	0.4861(3)	0.4016(1)	0.08474	0.06510	0.05100	0.00445	0.01483	-0.01101
C(73)	0.3359(4)	0.5987(4)	0.4001(2)	0.12182	0.07232	0.06461	0.01796	0.01183	-0.01239
C(74)	0.2313(4)	0.5772(5)	0.4249(2)	0.09243	0.11053	0.08246	0.03487	0.00378	-0.03329
C(75)	0.2127(3)	0.4466(5)	0.4513(2)	0.06659	0.12632	0.08943	0.01596	0.02249	-0.02826
C(76)	0.2966(3)	0.3341(4)	0.4531(2)	0.06360	0.09259	0.06884	0.00481	0.02346	-0.01590
C(81)	0.6992(2)	0.0613(3)	0.3766(1)	0.05141	0.05531	0.05598	0.00756	0.01873	0.00469
C(82)	0.7947(3)	0.0963(3)	0.4424(2)	0.05646	0.08237	0.06358	0.00627	0.01368	0.01172
C(83)	0.9188(3)	0.1379(4)	0.4426(2)	0.05501	0.09554	0.08191	0.00061	0.00650	0.00576
C(84)	0.9463(3)	0.1441(4)	0.3773(2)	0.05421	0.08584	0.10167	0.00206	0.03041	0.00546
C(85)	0.8521(3)	0.1095(4)	0.3121(2)	0.06487	0.08789	0.08593	0.00111	0.03787	0.00067
C(86)	0.7280(3)	0.0676(3)	0.3108(2)	0.05632	0.07361	0.06558	-0.00082	0.02694	-0.00326

Table 7.1 (contd.)

Atom	x	y	z	Atom	x	y	z
H(41)	0.1655	-0.0434	0.2893	H(61)	0.3456	0.2153	0.1795
H(42)	0.2952	-0.1016	0.2728	H(62)	0.4068	0.0578	0.2068
H(91)	0.0629	0.1888	0.2384	H(101)	0.1434	0.0862	0.1070
H(92)	0.1985	0.2714	0.2827	H(102)	0.2010	-0.0683	0.1422
H(93)	0.1328	0.2915	0.1935	H(103)	0.0640	-0.0095	0.1494
H(12)	0.5043	0.5032	0.3814	H(22)	0.7725	0.0915	0.4940
H(13)	0.3529	0.7024	0.3791	H(23)	0.9924	0.1653	0.4953
H(14)	0.1655	0.6645	0.4238	H(24)	0.0429	0.1766	0.3784
H(15)	0.1296	0.4275	0.4709	H(25)	0.8734	0.1141	0.2602
H(16)	0.2809	0.2284	0.4733	H(26)	0.6534	0.0403	0.2589
H(71)	0.5845	0.2761	0.4337	H(81)	0.5344	-0.0618	0.3343
H(72)	0.5090	0.1759	0.4766	H(82)	0.5773	-0.0397	0.4235

^a The temperature factor expression for the anisotropic atoms is

$$\exp[-2\pi^2(U_{11}h^2a^{*2} + U_{22}k^2b^{*2} + U_{33}l^2c^{*2} + 2U_{12}hka^*b^* + 2U_{13}hla^*c^* + 2U_{23}klb^*c^*)]$$

TABLE 7.2
ROOT MEAN SQUARE AMPLITUDES OF VIBRATION (\AA)

Atom	Minimum	Intermediate	Maximum
O(1)	0.208(3)	0.245(2)	0.272(2)
O(3)	0.198(3)	0.284(2)	0.325(3)
C(1)	0.192(3)	0.223(3)	0.229(4)
C(2)	0.200(3)	0.217(3)	0.233(4)
C(3)	0.209(4)	0.233(4)	0.255(3)
C(4)	0.217(4)	0.253(4)	0.291(4)
C(5)	0.219(4)	0.246(4)	0.274(4)
C(6)	0.209(3)	0.234(3)	0.271(4)
C(7)	0.209(3)	0.228(3)	0.253(4)
C(8)	0.220(4)	0.229(3)	0.259(3)
C(9)	0.235(4)	0.290(4)	0.316(4)
C(10)	0.230(4)	0.315(4)	0.358(4)
C(71)	0.180(4)	0.242(4)	0.270(4)
C(72)	0.212(4)	0.261(4)	0.306(4)
C(73)	0.234(4)	0.269(4)	0.381(5)
C(74)	0.234(5)	0.263(4)	0.420(5)
C(75)	0.240(5)	0.276(4)	0.388(5)
C(76)	0.235(4)	0.257(4)	0.320(4)
C(81)	0.213(4)	0.232(3)	0.250(4)
C(82)	0.227(4)	0.260(4)	0.297(4)
C(83)	0.227(4)	0.301(4)	0.319(4)
C(84)	0.225(4)	0.290(4)	0.322(4)
C(85)	0.228(4)	0.296(4)	0.299(4)
C(86)	0.222(4)	0.258(3)	0.274(4)

TABLE 7.3

BOND DISTANCES^a (Å)

O(1)-C(1)	1.210(3)	C(5)-C(9)	1.528(4)
O(3)-C(3)	<u>1.216(3)</u>	C(5)-C(10)	<u>1.530(4)</u>
	1.213(4)		1.529(1)
C(1)-C(6)	1.507(3)	C(7)-C(71)	1.506(3)
C(3)-C(4)	1.502(4)	C(8)-C(81)	<u>1.507(4)</u>
C(1)-C(2)	1.527(3)		1.506(1)
C(2)-C(3)	1.528(3)		
C(4)-C(5)	1.529(4)	C(2)-C(7)	1.546(3)
C(5)-C(6)	<u>1.527(4)</u>	C(2)-C(8)	1.585(3)
	1.52 (1)		
C(71)-C(72)	1.383(4)	C(81)-C(82)	1.385(4)
C(72)-C(73)	1.395(4)	C(82)-C(83)	1.400(4)
C(73)-C(74)	1.381(5)	C(83)-C(84)	1.379(4)
C(74)-C(75)	1.364(6)	C(84)-C(85)	1.370(4)
C(75)-C(76)	1.386(5)	C(85)-C(86)	1.395(4)
C(76)-C(71)	<u>1.400(4)</u>	C(86)-C(81)	<u>1.395(3)</u>
	1.39 (1)		1.39 (1)

^aThe figures in parentheses are e.s.d.'s in the last significant figure. Mean values are calculated using the expression

$$\bar{l} = \Sigma(l_i/\sigma_i^2)/\Sigma(1/\sigma_i^2)$$

The e.s.d. of the mean value is calculated as a root mean square deviation using the expression

$$\sigma(\bar{l}) = [\Sigma(\bar{l}-l_i)^2/(N-1)]^{1/2}$$

TABLE 7.4

BOND ANGLES^a (°)

C(1)-C(2)-C(3)	113.2(2)	C(4)-C(5)-C(9)	110.6(2)
C(6)-C(1)-C(2)	118.4(2)	C(4)-C(5)-C(10)	109.1(2)
C(2)-C(3)-C(4)	119.3(2)	C(6)-C(5)-C(9)	110.4(2)
C(3)-C(4)-C(5)	113.8(2)	C(6)-C(5)-C(10)	<u>109.0(2)</u>
C(5)-C(6)-C(1)	113.9(2)		109.8
C(4)-C(5)-C(6)	107.7(2)		
		C(9)-C(5)-C(10)	110.0(2)
C(4)-C(3)-O(3)	120.3(2)		
C(2)-C(3)-O(3)	120.1(2)	C(2)-C(7)-C(71)	116.2(2)
C(6)-C(1)-O(1)	121.0(2)	C(2)-C(8)-C(81)	<u>116.3(2)</u>
C(2)-C(1)-O(1)	<u>120.5(2)</u>		116.3
	120.5		
		C(7)-C(71)-C(72)	120.8(2)
C(3)-C(2)-C(7)	112.3(2)	C(7)-C(71)-C(76)	121.2(3)
C(3)-C(2)-C(8)	102.7(2)	C(8)-C(81)-C(82)	121.0(2)
C(1)-C(2)-C(7)	111.7(2)	C(8)-C(81)-C(86)	<u>119.5(2)</u>
C(1)-C(2)-C(8)	106.9(2)		120.6
C(7)-C(2)-C(8)	109.5(2)		

Table. 7.4 (contd.)

C(71)-C(72)-C(73)	121.3(3)	C(81)-C(82)-C(83)	120.0(3)
C(72)-C(73)-C(74)	119.6(3)	C(82)-C(83)-C(84)	120.1(3)
C(73)-C(74)-C(75)	119.8(3)	C(83)-C(84)-C(85)	120.1(3)
C(74)-C(75)-C(76)	121.1(3)	C(84)-C(85)-C(86)	120.6(3)
C(75)-C(76)-C(71)	120.3(3)	C(85)-C(86)-C(81)	119.8(3)
C(76)-C(71)-C(72)	<u>118.0(3)</u>	C(86)-C(81)-C(82)	<u>119.4(2)</u>
	120.0		120.0

^aAs for Table 7.3, but e.s.d.'s for the mean values were not calculated as they are much larger than an e.s.d. for an individual value.

TABLE 7.5

MEAN PLANES

Plane	Atoms through which mean plane is calculated
I	C(1), C(2), C(3)
II	C(1), C(3), C(4), C(6)
III	C(4), C(5), C(6)
IV	C(71), C(72), C(73), C(74), C(75), C(76)
V	C(81), C(82), C(83), C(84), C(85), C(86)

TABLE 7.6

NON-BONDED INTRAMOLECULAR DISTANCES (Å)

O(1)-C(7)	2.81	O(3)-C(7)	2.83
O(1)-C(8)	3.20	O(3)-C(8)	3.07
O(1)-C(72)	3.08	O(3)-C(76)	3.16
O(1)-C(81)	3.17		
O(1)-C(86)	3.20		

to 120° (range $118.0 - 121.3^\circ$). The exocyclic angles of the type C(7)-C(71)-C(72) are also close to 120° (range $119.5 - 121.2^\circ$). The angles around the quaternary carbon atoms, joining the phenyl groups to the cyclohexane ring (116.2 and 116.3°), deviate significantly from the ideal tetrahedral value. It must be assumed that this arises from the crowding of the phenyl groups by adjacent oxygen atoms. Table 7.6 summarizes the intra-molecular non-bonded contacts involving these atoms. This crowding is also indicated by the two bond lengths C(6)-C(2) and C(8)-C(2) at 1.546 and 1.585 \AA respectively. It appears that for the phenyl group bonded through atom C(8) angle deformation does not relieve all of the steric strain.

The ring geometry in the vicinity of the carbonyl groups can be rationalized in terms of the sp^2 hybridisation of atoms C(1) and C(3). The internal angles of the cyclohexane ring have been deformed in a systematic way to accommodate this effect. The angles at C(1) (118.4°) and C(3) (119.3°) are closer to 120° than for acetone⁵⁵ (116.4°), 1,4-cyclohexane dione^{56,57} (116.2°), and 4,4-diphenylcyclohexanone⁵⁸ (116.8°). The angles at C(2), C(4) and C(6) have also been increased beyond the tetrahedral angle to the values of 113.2 , 113.8 and 113.9° respectively. The angle of C(5) is

reduced at 107.7° , an effect observed before which is probably a direct result of the enlarged angles at C(1) and C(3).

The bonds C(1)-C(6) and C(3)-C(4) are lengthened with respect to the other four bonds within the ring. A shortening of one of the C-C bonds to a carbonyl group has been observed in 1,4-cyclohexanedione⁵⁶ ($1.505\overset{\text{O}}{\text{\AA}}$) and 4,4-diphenylcyclohexanone⁵⁷ ($1.465\overset{\text{O}}{\text{\AA}}$), which are similar to the values of 1.502 and 1.507 observed in this compound.

The atoms C(1), C(3), C(4) and C(6) are essentially planar (Plane II) with the opposing bonds slightly skewed. Atoms C(1) and C(4) are both above the plane by $0.005\overset{\text{O}}{\text{\AA}}$ and atoms C(3) and C(6) are both below the plane by the same amount. It may also be noted that O(1) lies further above this plane at $0.21\overset{\text{O}}{\text{\AA}}$ than does O(3) which is $0.13\overset{\text{O}}{\text{\AA}}$ above the plane. This may be a result of steric interaction between the carbonyl oxygen atom and a phenyl group.

The results of this structural analysis have shown that the postulated structure of Wynberg is incorrect for this compound. If it can be assumed that solution and solid state conformations approximate to each other then the original assignments of the nuclear magnetic resonance spectrum are incorrect.

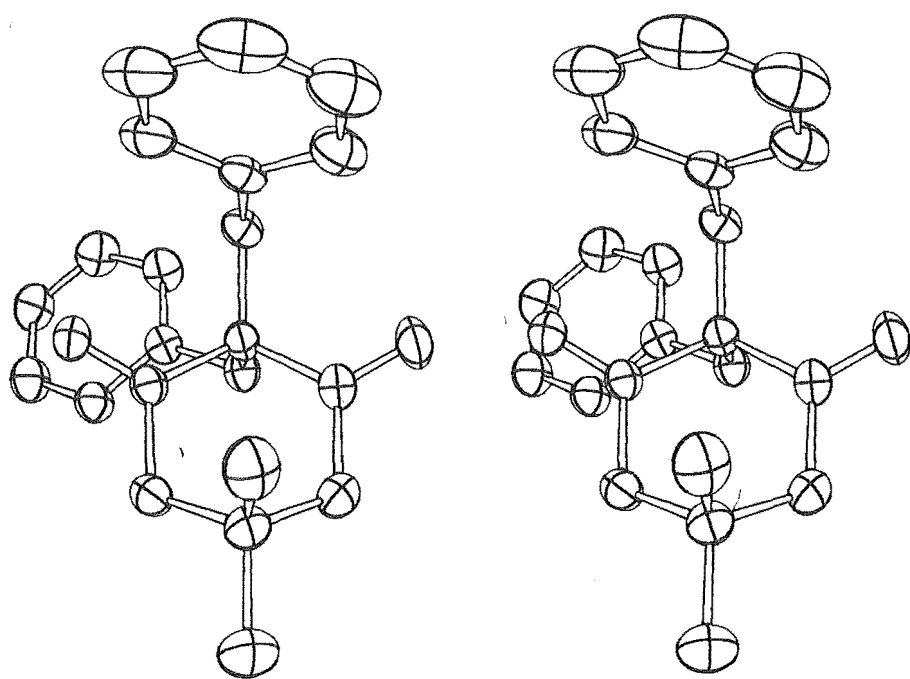


Figure 7.2 A Stereoscopic View of $C_{22}H_{24}O_2$

The phenyl group suggested to cause the majority of the shielding of the methyl groups in Wynberg's¹¹ model, corresponding to C(9) and C(10) in this compound, could not be the same as that which causes the shielding in dibenzyl dimedone. This is because the phenyl group in question, that bonded to C(8) in this structure, adopts a position to one side of the cyclohexane ring and not directly beneath it. In fact the calculated values for shielding constants in this compound are consistent with the observed data⁵⁹.

This structure has provided a model conformation on which to base the interpretation of nuclear magnetic resonance spectra for similar compounds.

CHAPTER VIII

Conclusion

It was not until the work described in this thesis had been completed, that I felt able to approach a problem with some certainty that its solution would be forthcoming using the direct methods described in Chapter III. Although I have been successful with the structural analyses that I have completed, the methods used are still far from being generally applicable.

My first serious attempt at applying the symbolic addition procedure was in the solution of the structure of 4 α -t-butyl-cyclohexane-1 β ,2 β -diol, described in Chapter V. As a structure in a triclinic space group had not been successfully solved with symbolic addition in this laboratory, there was some uncertainty as to where the errors (incorrect assignments of structure factor signs) were occurring. There were two stages where problems could arise: firstly with the determination of symbolic signs for those data with large $|E|$ values, and secondly, and perhaps more important, the determination of absolute signs for all those data to be included in the subsequent Fourier synthesis. It was felt that if the $|E|$ limit was kept high enough the possibility of errors occurring in the first stage

could be ignored. It then had to be decided, to what degree attempts could be made to determine absolute signs for data with lower $|E|$ values. As the number of symbols whose signs had to be determined was usually four, giving fifteen possible Fourier syntheses to be evaluated, it was desirable to determine some order in which this should be done. With program SAP there was no such facility. The $|E|$ limit for the second stage was chosen so that there were ten to fifteen signed data for each non-hydrogen atom in the asymmetric unit.

With this low $|E|$ limit it was found that no chemically reasonable structure appeared. This was attributed to the number of incorrect sign determinations during the second stage of the symbolic addition procedure. By raising the $|E|$ limit, it was felt that not enough data was being used to give a Fourier synthesis, with adequate resolution.

It was not until my implementation of program DPHASE, that a reliable method was found to extend the sign set (increase the number of data for which absolute signs have been determined), and also to evaluate a reliability index in the R-Karle value. With the application of the tangent formula the structure was readily solved. The transfer between the two methods took place after the determination of

symbolic signs for those data with $|E| \geq 1.7$, an acceptably high value.

Experience with direct methods applied to non-centrosymmetric crystals was first obtained with the solution of the structure of $C_{10}H_{16}SO_3(B)$, described in Chapter VI. To initiate the phasing procedure, symbolic phases were determined by hand for 30 to 40 data having $|E| \geq 1.7$, after determination of the origin and assignment of the enantiomorph. These first steps are the ones most prone to error. It would not be unusual to start a number of times with different choices for the origin defining reflections. Again, once trial values for the symbols can be determined, the tangent formula can be used to both refine phases and increase the number of data whose phases have been estimated. An R-Karle value of 0.2-0.3 would usually indicate a correct solution, although the phase set with the lowest R-Karle value would not necessarily be the correct one.

Once a structural fragment has been correctly located, the rest of a structure can usually be readily located by reiterative use of the tangent formula as described by Karle⁶⁰. However, problems can still arise with space groups like $P2_1$, with a phase set refining to reflect a centrosymmetric distribution of

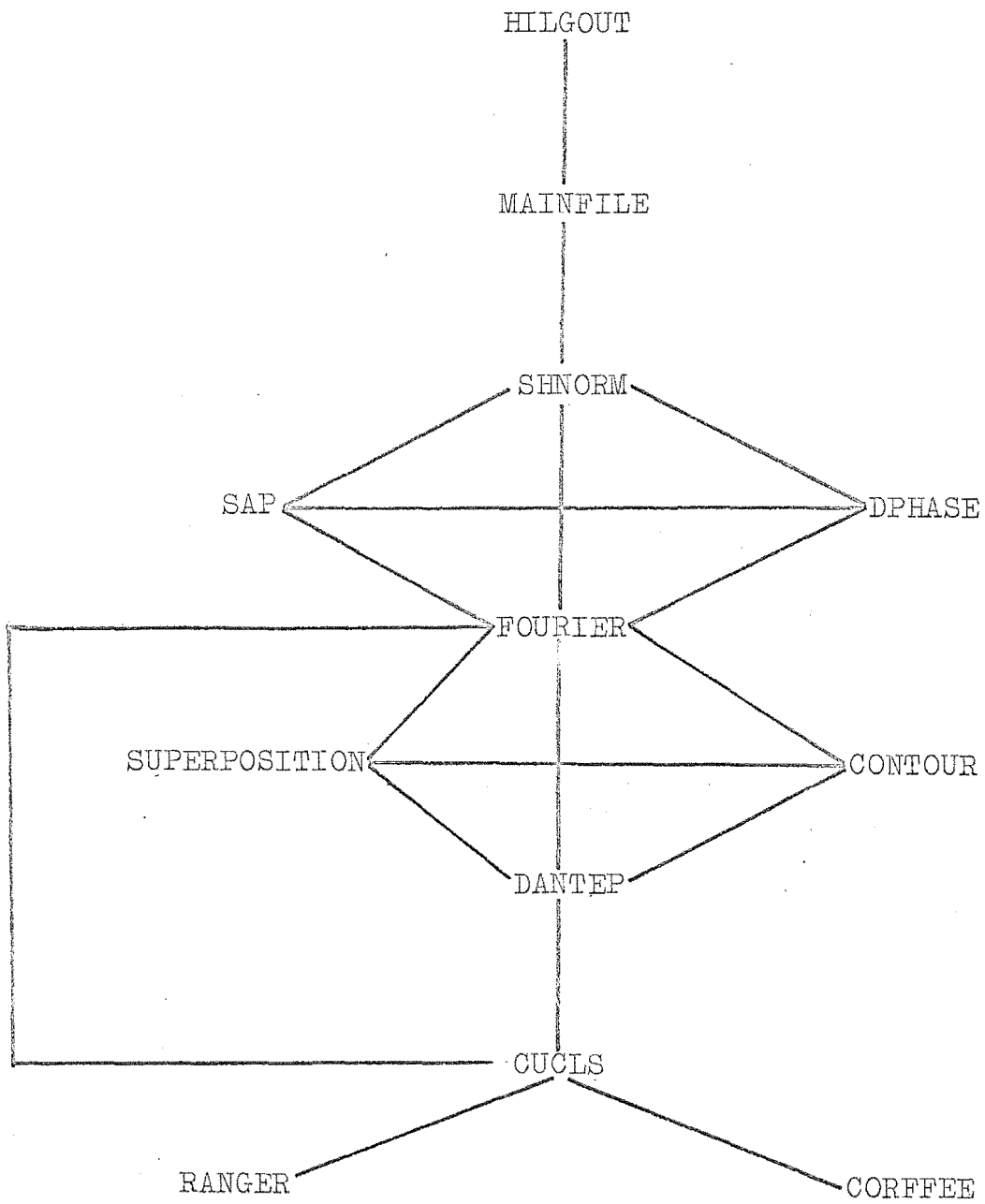
electron density, hence precluding a correct structural solution.

In conclusion, the success of direct methods appears to be dependent upon such factors as space group, the completeness of the data set, and the intuition of the user. For those centrosymmetric structures for which symbolic addition does not produce a unique solution, the tangent formula can be almost guaranteed to work. With noncentrosymmetric structures the possibility of error is much higher and hence a more sophisticated decision sequence is required. A procedure recently described⁶¹, where the possibility of one or more errors in the stepwise determination of phases is anticipated and allowed for, provides such a sequence. This approach could greatly improve the power of direct phasing techniques.

Direct methods are competitive with other techniques for structure solution, as they give a more complete answer, more quickly, with a consequent saving of expensive computing time.

FIGURE A.1

COMPUTING SYSTEM



APPENDIX AComputing System

The set of crystallographic programs used during the course of this work is large, and was obtained from a number of sources. It is intended to outline here, how each program was used and to indicate its origin. Many changes have been made to some programs, partly to incorporate features of a number of different programs, but mainly because of hardware restrictions. The available computer was an IBM 360/44 with 128K bytes of core storage and two million characters of disk storage.

Some details of the main programs used, shown in Figure A.1, are as follows:

HILGOUT is the processing program for data collected on the diffractometer; output from this instrument is on paper tape in a free format. This program is also used to average the intensities of crystallographically equivalent reflections. Some parts of HILGOUT are based on programs DRED (J.F. Blount) and PICKOUT (R.J. Doedens).

SHNORM estimates overall scale and temperature factors using the Wilson-plot method, prior to calculation of coefficients for a sharpened Patterson or normalized structure factors. It also produces a

file of triplets of reflections which satisfy the Σ_2 relationship for use by program DPHASE. SHNORM was derived from parts I to III of NRC-5⁶² (C.P. Huber and F.R. Brisse) and also some of Part II of NRC-4⁶³ (S.R. Hall).

SAP comprises parts III and IV of the revised version of NRC-4⁶³ (S.R. Hall and F.R. Ahmed). It attempts to determine phases for normalized structure factors of centrosymmetric space groups by use of the symbolic addition procedure.

DPHASE attempts to estimate structure factor phases of centrosymmetric and noncentrosymmetric structures using the Σ_2 relationship and the tangent formula. It is derived from parts IV and V of NRC-5.

FOURIER, the program for calculation of Fourier summations, is a rewritten version of program FORDAP (A. Zalkin). The answers can be plotted on the line-printer using a set of alphameric characters, or can be plotted on a Calcomp incremental plotter using program CONTOUR by connecting the points of equal electron density for as many levels as are required. Another improvement was incorporation of a routine to find the local maxima of an electron density map by interpolation at points on a three-dimensional grid.⁶⁴

DANTEP is used for distance and angle calculations, and for production of crystal structure diagrams on the line-printer and on the Calcomp plotter; it is a modified version of C.K. Johnson's ORTEP⁶⁵. Communication with the plotter was through large decks of punched cards, hence the line-printer was used as frequently as possible.

CUCLS calculates structure factors and performs cycles of full-matrix least-squares refinement; it is a highly modified version of program ORFLS⁶⁶. The program contains routines for the application of geometric constraints^{53,54} based, for the most part, on program NUGLS, a version of ORFLS modified by J.A. Ibers and R.J. Doedens. The program is also able to treat crystal decomposition according to the method outlined by Ibers⁶⁷, and secondary extinction using the method of Zachariasen³⁷ as incorporated by Larson³⁸.

APPENDIX BStructure Factor Tables

	<u>Title</u>	<u>Page</u>
Table B.1	Observed and Calculated Structure Amplitudes in Electrons for $[\text{Co}_3(\text{CO})_9]_2$	112
Table B.2	Observed and Calculated Structure Amplitudes (x10) in Electrons for $\text{C}_{10}\text{H}_{20}\text{O}_2$	113
Table B.3	Observed and Calculated Structure Amplitudes (x10) in Electrons for $\text{C}_{10}\text{H}_{16}\text{SO}_3(\text{A})$	114
Table B.4	Observed and Calculated Structure Amplitudes (x10) in Electrons for $\text{C}_{10}\text{H}_{16}\text{SO}_3(\text{B})$	115
Table B.5	Observed and Calculated Structure Amplitudes (x10) in Electrons for $\text{C}_{22}\text{H}_{24}\text{O}_2$	116

[illegible]

REFERENCES

- 1 G. Allegra, E.M. Peronaci and R. Ercoli, Chem. Comm., 549 (1966).
- 2 P.W. Sutton and L.F. Dahl, J. Amer. Chem. Soc., 89, 261 (1967).
- 3 B.H. Robinson, J.L. Spencer and R. Hodges, Chem. Comm., 1480 (1968).
- 4 R.J. Dellaca, B.R. Penfold, B.H. Robinson, W.T. Robinson and J.L. Spencer, Inorg. Chem., 9, 2204 (1970).
- 5 R.J. Dellaca and B.R. Penfold, Inorg. Chem., 10, 1269 (1971).
- 6 G. Allegra and S. Valle, Acta Cryst., B25, 107 (1969).
- 7 R.J. Dellaca, B.R. Penfold, B.H. Robinson, W.T. Robinson and J.L. Spencer, Inorg. Chem., 9, 2197 (1970).
- 8 'Studies in Carbonium Ion Chemistry', G.R. Little, Ph.D. Thesis, University of Canterbury (1971).
- 9 J.M. Coxon, E. Dansted, M.P. Hartshorn and K.E. Richards, Tetrahedron, 24, 1193 (1968).
- 10 M.D. Brice, J.M. Coxon, E. Dansted, M.P. Hartshorn and W.T. Robinson, Chem. Comm., 356 (1969).

- 11 H.A.P. De Jongh and H. Wynberg, *Tetrahedron*, 21, 515 (1965).
- 12 M. Renninger, *Z. Krist.*, 97, 107 (1937).
- 13 W.R. Busing and H.A. Levy, ORNL-4054, Oak Ridge National Laboratory, U.S.A. (1967).
- 14 W.R. Busing, Paper I1, International Summer School on Crystallographic Computing, Ottawa, Canada (1969).
15. T.C. Furnas, 'Single Crystal Orienter Instruction Manual', General Electric Co., Milwaukee, U.S.A. (1957).
- 16 P.W.R. Corfield, R.J. Doedens and J.A. Ibers, *Inorg. Chem.*, 6, 197 (1967).
- 17 D.F. Grant, R.C.G. Killeen and J.L. Lawrence, *Acta Cryst.*, B25, 374 (1969).
- 18 D.W.J. Cruickshank in 'Computing Methods in Crystallography', Ed., J.S. Rollet, Pergamon, Oxford, p.114 (1965).
- 19 W.T. Robinson and J.A. Ibers, *Inorg. Chem.*, 6, 1208 (1967).
- 20 J. Karle and I.L. Karle, *Acta Cryst.*, 21, 849 (1966).
- 21 A.J.C. Wilson, *Nature*, 150, 151 (1942).
- 22 H. Hauptmann and J. Karle, in 'Solution of the Phase Problem. I. The Centrosymmetric Crystal'. A.C.A.

Monograph No. 3. Pittsburgh: Polycrystal Book Service.

- 23 J. Karle, Paper A1, International Summer School on Crystallographic Computing, Ottawa, Canada (1969).
- 24 H. Hauptmann and J. Karle, Acta Cryst., 9, 45 (1956).
- 25 J. Karle and H. Hauptmann, Acta Cryst., 14, 217 (1961).
- 26 J. Karle and H. Hauptmann, Acta Cryst., 9, 635 (1956).
- 27 J. Karle, Acta Cryst., B24, 182 (1968).
- 28 D.T. Cromer and J.T. Waber, Acta Cryst., 18, 104 (1965).
- 29 D.T. Cromer and J.B. Mann, Acta Cryst., A24, 321 (1968).
- 30 R.F. Stewart, E.R. Davidson and W.T. Simpson, J. Chem. Phys., 42, 3175 (1965).
- 31 J.A. Ibers and W.C. Hamilton, Acta Cryst., 17, 781 (1964).
- 32 D.T. Cromer, Acta Cryst., 18, 17 (1964).
- 33 J.M. Bijvoet, A.F. Peerdman and A.J. Van Bommel, Nature, 168, 271 (1951).
- 34 A.L. Patterson, Z. Krist., A90, 517 (1935).
- 35 D. Harker, J. Chem. Phys., 4, 381 (1936).

- 36 M.J. Buerger in 'Vector Space', New York, John Wiley & Sons, Inc., Chapter 7.
- 37 W.H. Zachariasen, *Acta Cryst.*, 23, 558 (1967).
- 38 A.C. Larson in 'Crystallographic Computing', Ed., F.R. Ahmed, Munksgaard, Copenhagen, 1970, p.291.
- 39 F. Klanberg, W.B. Askew and L.J. Guggenberger, *Inorg. Chem.*, 7, 2265 (1968).
- 40 B.H. Robinson, Private Communication.
- 41 Chem. Soc., Special Publication, No. 18 (1965).
- 42 M.D. Brice, R.J. Dellaca, B.R. Penfold and J.L. Spencer, *Chem. Comm.*, 72 (1971).
- 43 M.D. Brice, B.R. Penfold, W.T. Robinson and S.R. Taylor, *Inorg. Chem.*, 9, 362 (1970).
- 44 C.R. Hubbard, and R.A. Jacobson, in a Research and Development Report for the United States Atomic Energy Commission, distributed according to the category Chemistry(UC-4) as listed in TID-4500. 'A Fortran IV Crystallographic System of Programs for Generalized Superpositions'.
- 45 I.N. Rabinowitz and J. Kraut, *Acta Cryst.*, 17, 159 (1964).
- 46 G.A. Jeffrey and H.S. Kim, *Acta Cryst.*, B27, 1812 (1971).
- 47 C. Pedone, E. Benedetti and G. Allegra, *Acta Cryst.*, B26, 933 (1970).

- 48 S.T. Rao and M. Sundaralingam, Acta Cryst., B25,
2509 (1969).
- 49 G.C. Pimentel, Private Communication.
- 50 'The Tangent Formula Program for the X-Ray Analysis
of Noncentrosymmetric Crystals', S.A. Brenner and
P.H. Gum, NRL Report 6697, Naval Research Laboratory,
Washington, D.C.
- 51 'Rearrangements in the Monoterpene Series', E.
Dansted, Ph.D. Thesis, University of Canterbury
(1968).
- 52 J.W.L. Van Oyen, R.C.D.E. Hasekamp, G.C. Verschoor
and C. Romers, Acta Cryst., B24, 1471 (1968).
- 53 S.J. La Placa and J.A. Ibers, Acta Cryst., 18, 511
(1965).
- 54 R.J. Doedens, Paper E3, International Summer School
on Crystallographic Computing, Ottawa, Canada
(1969).
- 55 J.D. Swalen and C.C. Costain, J. Chem. Phys., 31,
1562 (1959).
- 56 A. Mossel and C. Romers, Acta Cryst., 17, 1217
(1964).
- 57 P. Groth and O. Hassel, Acta Chem. Scand., 18, 923
(1964).
- 58 J.B. Lambert, R.E. Carhart and P.W.R. Corfield, J.
Amer. Chem. Soc., 91, 3567 (1969).
- 59 M.H.G. Munro, Private Communication.

- 60 J. Karle, Paper A4, International Summer School on Crystallographic Computing, Ottawa, Canada (1969).
- 61 G. Germain, P. Main and M.M. Woolfson, Acta Cryst., B26, 274 (1970).
- 62 C.P. Huber and F.R. Brisse, NRC-5, National Research Council, Ottawa, Canada (1970).
- 63 S.R. Hall and F.R. Ahmed, NRC-4, National Research Council, Ottawa, Canada (1968).
- 64 J.S. Rollett in 'Computing Methods in Crystallography', Ed. J.S. Rollett, Pergamon, Oxford, p.35 (1965).
- 65 C.K. Johnson, ORNL-3794, Oak Ridge National Laboratory, U.S.A. (1965).
- 66 W.R. Busing, K.O. Martin and H.A. Levy, ORNL-TM-305, Oak Ridge National Laboratory, U.S.A. (1962).
- 67 J.A. Ibers, Acta Cryst., B25, 1667 (1969).